Electronic Supplementary Material (ESI) for Journal of Materials Chemistry A.
This journal is © The Royal Society of Chemistry 2024

# Electronic supplementary information

**Sandwiching high energy frameworks by taking advantage of π-philic molecular recognition**

Jatinder Singh[a], Richard J. Staples[b], Magdalena Fabin[a,c], Jean'ne M. Shreeve[a,*]

[a] Department of Chemistry, University of Idaho, Moscow, Idaho, 83844-2343, United States.

[b] Department of Chemistry, Michigan State University, East Lansing, Michigan 48824, United States.

[c] Department of Physical Chemistry and Technology of Polymers, Silesian University of Technology, 44-100 Gliwice, Poland.

**Corresponding Author**

**Jean'ne M. Shreeve** − Department of Chemistry, University of Idaho, Moscow, Idaho 83844-2343, United States.

Email: jshreeve@uidaho.edu; Fax: (+1) 208-885-5173.

**Table of contents**

## Section 1. Experimental section

### Section S1.1. Caution!

All compounds should be synthesized in milligram amounts. The new compounds are energetic materials which show increased sensitivities toward various stimuli (e.g., higher temperatures, impact, and friction). Proper safety precautions such as leather gloves, face shield, and eye protection must be taken at all times while synthesizing and handling these materials.

### Section S1.2. General methods

All reagents (analytical grade) were purchased from AK Scientific or VWR and were used as supplied. $^{1}H$, $^{13}C$ NMR, $^{14}N$ NMR and $^{15}N$ NMR spectra were recorded using a 500 MHz (Bruker AVANCE 500) NMR spectrometer operating at 500.19, 125.78, 36.14, and 50.69 MHz, respectively. Chemical shifts in the $^{1}H$ and $^{13}C$ NMR spectra are reported relative to $Me_4Si$ and $^{15}N$ NMR spectra to $MeNO_2$ as an external standard. Abbreviations for multiplicities and descriptors are: s = singlet, br = broad signal, m = multiplet (denotes complex pattern), and q = quartet. The decomposition points (onset temperature) were obtained on a differential scanning calorimeter (TA Instruments Company, Model: Q2000) at a scan rate of 5 °C $min^{-1}$. Infrared spectra were recorded on a FT-IR spectrometer (Thermo Nicolet AVATAR 370) as thin films using KBr plates. The room temperature densities were measured at 25 °C by employing a gas pycnometer (Micromeritics AccuPyc II 1340). The impact and friction sensitivities were determined by using a standard BAM drop hammer and BAM friction tester. Elemental analyses were carried out on a Vario Micro cube Elementar Analyser.

### General procedure for the synthesis of TATOT salts

Compounds **2**-**9** and their corresponding silver or ammonium salts were prepared following literature procedures.[1-8] $Ag^+$ or $NH_4^+$ salts of compounds **2**, **3**, **4**, **5**, **6**, **7**, **8** and **9** (1 eq.) were added to a suspension of **TATOT.HCl** (2 eq.) in $H_2O$ (30 mL). The reaction mixture was heated to 50 °C on a magnetic stirrer with oil bath for 30 min. The precipitate was collected by filtration to give the product, which was purified further by washing with $H_2O$ (3 x 10 mL).

**ISEM-2:** Physical description: Yellow solid. Isolated yield: (0.55 g, 92%); $T_{dec.}$ (onset) = 189 °C; $^{1}$H NMR (500 MHz, $d_6$-DMSO): 13.37 (br, 2H), 8.11 (s, 4H), 7.20 (s, 4H), 5.76 (s, 4H); $^{13}$C NMR (125 MHz, $d_6$-DMSO): 160.1, 152.0, 147.4, 141.2, 132.7; IR ($\tilde{\nu}$, $cm^{-1}$): 3412, 3253, 1702, 1654, 1618, 1561, 1518, 1409, 1284, 1212, 1075; Elemental analysis: Calcd (%) for $C_{10}H_{14}N_{24}O_8$ (598.37): C, 20.07; H, 2.36; N, 56.18; Found: C, 19.94; H, 2.61; N, 55.91.

**ISEM-3:** Physical description: Red solid. Isolated yield: (0.45 g, 88%); $T_{dec.}$ (onset) = 238 °C; $^{1}$H NMR (500 MHz, $d_6$-DMSO): 10.42 (br, 2H), 7.74 (s, 4H), 7.08 (s, 4H), 5.75 (s, 4H); $^{13}$C NMR (125 MHz, $d_6$-DMSO): 163.9, 160.0, 147.8, 141.6; IR ($\tilde{\nu}$, $cm^{-1}$): 3401, 3255, 1700, 1683, 1650, 1616, 1562, 1519, 1458, 1421, 1384, 1359, 1237, 1072, 1040, 971, 890, 848, 775, 722, 708; Elemental analysis: Calcd (%) for $C_8H_{14}N_{24}O_4$ (510.36): C, 18.83; H, 2.76; N, 65.87; Found: C, 18.45; H, 3.33; N, 65.52.

**ISEM-4:** Physical description: Yellow solid. Isolated yield: (0.58 g, 92%); $T_{dec.}$ (onset) = 203 °C; $^{1}$H NMR (500 MHz, $d_6$-DMSO): 13.71 (br, 2H), 8.09 (s, 4H), 7.17 (s, 4H), 5.74 (s, 4H); $^{13}$C NMR (125 MHz, $d_6$-DMSO): 160.2, 147.5, 141.3, 137.3, 128.0, 124.6; IR ($\tilde{\nu}$, $cm^{-1}$): 3411, 3320, 2917, 2851, 1700, 1654, 1562, 1510, 1458, 1430, 1384, 1229, 1192, 1122, 1041, 959, 822, 708; Elemental analysis: Calcd (%) for $C_{11}H_{15}N_{23}O_{10}$ (629.38): C, 20.99; H, 2.40; N, 51.19; Found: C, 20.85; H, 2.34; N, 51.47.

**ISEM-5:** Physical description: Light yellow solid. Isolated yield: (0.56 g, 73%); $T_{dec.}$ (onset) = 226 °C; $^{1}$H NMR (500 MHz, $d_6$-DMSO): 7.75 (s, 4H), 7.08 (s, 4H), 5.73 (s, 4H); $^{13}$C NMR (125 MHz, $d_6$-DMSO): 172.0, 159.9, 147.7, 141.5; IR ($\tilde{\nu}$, $cm^{-1}$): 3313, 3109, 2137, 1689, 1656, 1562, 1510, 1450, 1417, 1384, 1119, 1058, 850 ; Elemental analysis: Calcd (%) for $C_8H_{14}N_{26}$ (474.37): C, 20.26; H, 2.97; N, 76.77; Found: C, 20.34; H, 3.85; N, 75.94.

**ISEM-6:** Physical description: Light yellow solid. Isolated yield: (0.50 g, 85%); $T_{dec.}$ (onset) = 225 °C; $^{1}$H NMR (500 MHz, $d_6$-DMSO): 13.31 (br, 2H), 8.17 (s, 4H), 7.21 (s, 4H), 5.76 (s, 4H); $^{13}$C NMR (125 MHz, $d_6$-DMSO): 160.3, 159.6, 147.6, 141.3, 121.8; IR ($\nu$, $cm^{-1}$): ; Elemental analysis: Calcd (%) for $C_{10}H_{14}N_{22}O_9$ (586.36): C, 20.48; H, 2.41; N, 52.55; Found: C, 20.47; H, 2.60; N, 52.82.

**ISEM-7:** Physical description: White solid. Isolated yield: (0.49 g, 87%); $T_{dec.}$ (onset) = 268 °C; $^{1}$H NMR (500 MHz, $d_6$-DMSO): 8.15 (s, 4H), 7.20 (s, 4H), 5.76 (s, 4H); $^{13}$C NMR (125 MHz, $d_6$-DMSO): 166.0,

160.1, 148.3, 147.4, 141.2; IR ($\tilde{\nu}$, $cm^{-1}$): 3453, 3207, 1688, 1651, 1558, 1521, 1497, 1428, 1281, 1245, 1160, 1077, 1021, 973, 912, 837, 777, 730; Elemental analysis: Calcd (%) for $C_{10}H_{14}N_{24}O_6$ (566.38): C, 21.21; H, 2.49; N, 59.35; Found: C, 21.50; H, 2.34; N, 60.15.

**ISEM-8:** Physical description: White solid. Isolated yield: (0.50 g, 88%); $T_{dec.}$ (onset) = 269 °C; $^1$H NMR (500 MHz, $d_6$-DMSO): 13.30 (br, 2H), 8.17 (s, 4H), 7.21 (s, 4H), 5.77 (s, 4H); $^{13}$C NMR (125 MHz, $d_6$-DMSO): 175.4, 160.3, 160.1, 147.4, 141.1; IR ($\tilde{\nu}$, $cm^{-1}$): 3402, 3256, 3117, 1698, 1682, 1650, 1616, 1580, 1519, 1486, 1465, 1449, 1412, 1385, 1315, 1294, 1270, 1256, 1232, 1181, 1063, 1049, 995, 972, 957, 850, 775, 759, 749, 722, 709; Elemental analysis: Calcd (%) for $C_{10}H_{14}N_{24}O_6$ (566.38): C, 21.21; H, 2.49; N, 59.35; Found: C, 21.42; H, 2.85; N, 59.06.

**9-TATOT:** Physical description: Yellow solid. Isolated yield: (0.26 g, 78%); $T_{dec.}$ (onset) = 129 °C; $^1$H NMR (500 MHz, $d_6$-DMSO): 13.26 (br, 2H), 8.17 (s, 4H), 7.21 (s, 4H), 5.76 (s, 4H); $^{13}$C NMR (125 MHz, $d_6$-DMSO): 160.1, 147.9, 147.4, 141.1, 113.7; Elemental analysis: Calcd (%) for $C_6H_7N_{15}O_4$ (353.22): C, 20.40; H, 2.00; N, 59.48; Found: C, 20.07; H, 2.48; N, 58.72.

## Section S2. X-ray crystallography details and crystallographic data

### Section S2.1. Data collection

Crystals with suitable dimensions were mounted on a nylon loop with Paratone oil. Data were collected using a XtaLAB Synergy, Dualflex, HyPix diffractometer equipped with an Oxford Cryosystems low-temperature device, operating at T = 99.9(4) K. The structures were solved with the ShelXT[11] solution program using dual methods and by using Olex2.[12] The model was refined with ShelXL[13] using full matrix least squares minimization on $F^2$. The thermal ellipsoid and packing diagrams of X-ray structures in the main article and supplementary material are plotted using Diamond 3.2 software.

### Section S2.2. Crystal structures and crystallographic data.

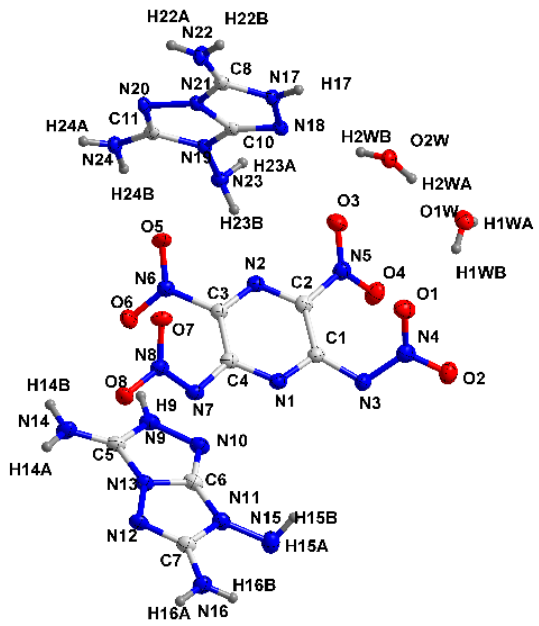


**Figure S1:** Thermal ellipsoid plot for **ISEM-2•$H_2O$**. Thermal ellipsoids are drawn at 50% probability level. Data collected at 100 K. CCDC # 2345095.

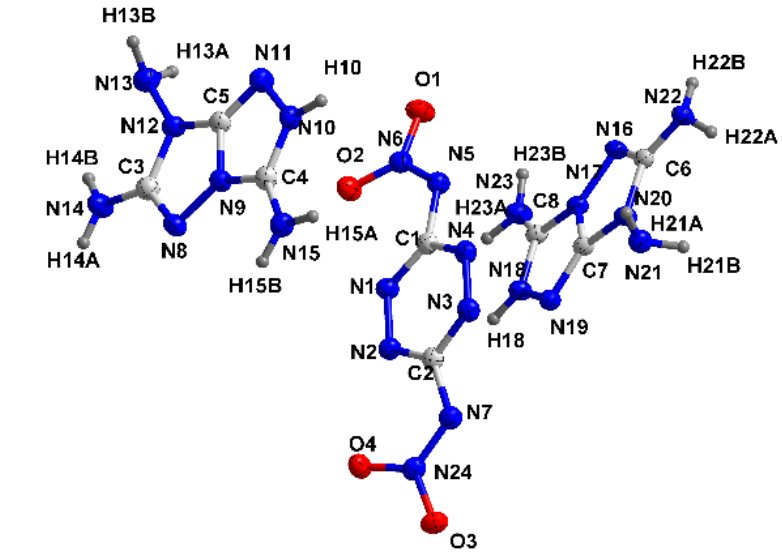


**Figure S2:** Thermal ellipsoid plot for **ISEM-3**. Thermal ellipsoids are drawn at 50% probability level. Data collected at 100 K. CCDC # 2345096.

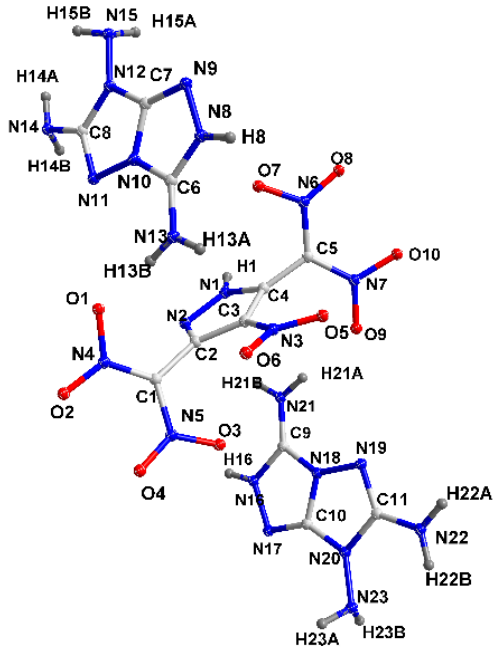


**Figure S3:** Thermal ellipsoid plot for **ISEM-4**. Thermal ellipsoids are drawn at 50% probability level. Data collected at 100 K. CCDC # 2345097.

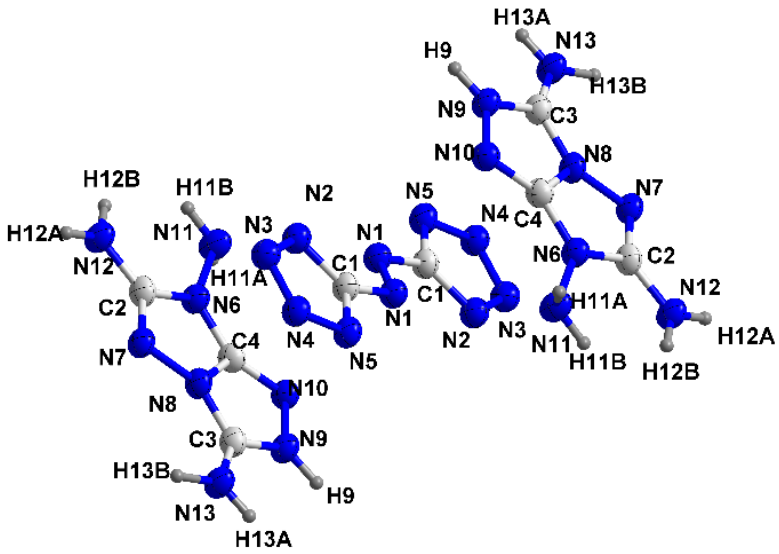


**Figure S4:** Thermal ellipsoid plot for **ISEM-5**. Thermal ellipsoids are drawn at 50% probability level. Data collected at 100 K. CCDC # 2345098.

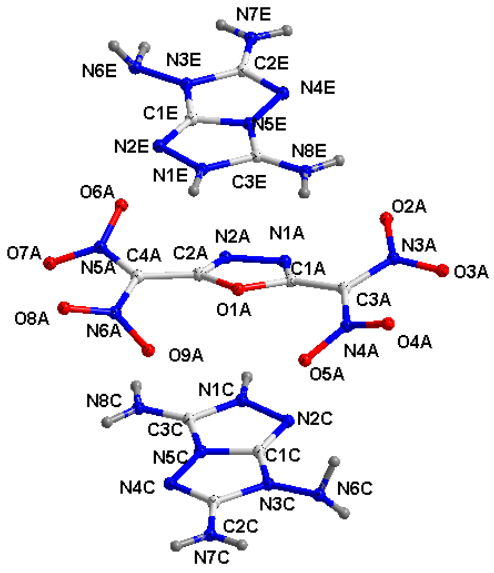


**Figure S5:** Thermal ellipsoid plot for **ISEM-6**. Thermal ellipsoids are drawn at 50% probability level. Data collected at 100 K. CCDC # 2350606.

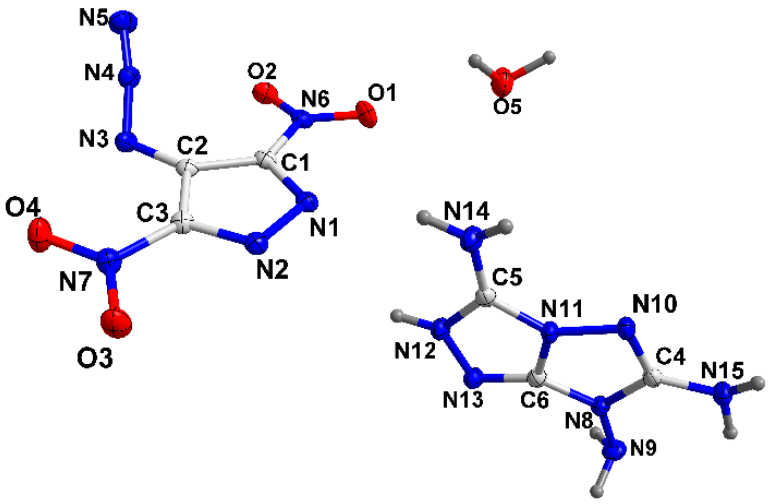


**Figure S6:** Thermal ellipsoid plot for **9-TATOT•$H_2O$**. Thermal ellipsoids are drawn at 50% probability level. Data collected at 100 K. CCDC # 2345099.

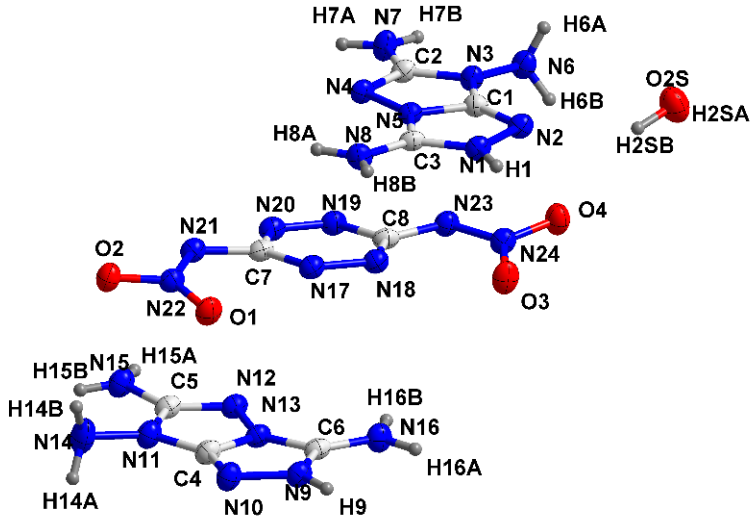


**Figure S7:** Thermal ellipsoid plot for **ISEM-3•$H_2O$**. Thermal ellipsoids are drawn at 50% probability level. Data collected at 100 K. CCDC # 2346398.

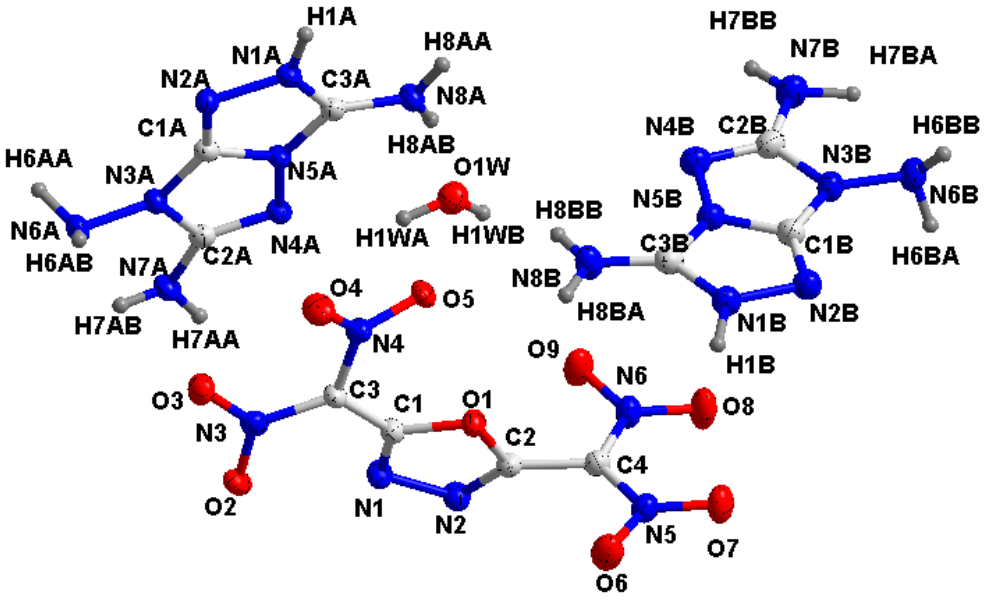


**Figure S8:** Thermal ellipsoid plot for **ISEM-6•$H_2O$**. Thermal ellipsoids are drawn at 50% probability level. Data collected at 100 K. CCDC # 2350679.

**Table S1:** Crystallographic data for **ISEM-2**, **ISEM-3**, **ISEM-4**, and **ISEM-5**.

| **Compound** | **ISEM-2** | **ISEM-3** | **ISEM-4** | **ISEM-5** |
|---|---|---|---|---|
| CCDC # | 2345095 | 2345096 | 2345097 | 2345098 |
| Formula | $C_{10}H_{18}N_{24}O_{10}$ | $C_8H_{14}N_{24}O_4$ | $C_{11}H_{15}N_{23}O_{10}$ | $C_8H_{12}N_{26}$ |
| $D_{calc.}$/ g cm$^{-3}$ | 1.758 | 1.808 | 1.862 | 1.674 |
| $m$/mm$^{-1}$ | 1.352 | 1.301 | 1.428 | 1.115 |
| Formula Weight | 634.48 | 510.43 | 629.46 | 472.44 |
| Color | yellow | red | yellow | yellow |
| Shape | needle-shaped | needle-shaped | needle-shaped | needle-shaped |
| Size/mm$^3$ | 0.25×0.04×0.01 | 0.19×0.07×0.02 | 0.37×0.09×0.05 | 0.14×0.04×0.02 |
| $T$/K | 100.00(10) | 99.98(12) | 99.97(13) | 100.00(14) |
| Crystal System | monoclinic | monoclinic | monoclinic | triclinic |
| Flack Parameter | - | - | 0.6(8) | - |
| Hooft Parameter | - | - | -0.30(10) | - |
| Space Group | $P2_1/c$ | $P2_1/n$ | $Pc$ | $P$-1 |
| $a$/Å | 19.9556(6) | 19.8933(7) | 11.8497(4) | 6.5508(8) |
| $b$/Å | 5.43943(16) | 4.99426(12) | 6.69000(10) | 6.7141(8) |
| $c$/Å | 22.8384(6) | 20.8330(7) | 15.2054(5) | 11.4242(9) |
| $\alpha$/° | 90 | 90 | 90 | 89.787(8) |
| $\beta$/° | 104.712(3) | 115.073(4) | 111.346(4) | 78.702(9) |
| $\gamma$/° | 90 | 90 | 90 | 72.292(11) |
| V/Å$^3$ | 2397.77(13) | 1874.77(12) | 1122.71(6) | 468.54(9) |
| $Z$ | 4 | 4 | 2 | 1 |
| $Z'$ | 1 | 1 | 1 | 0.5 |
| Wavelength/Å | 1.54184 | 1.54184 | 1.54184 | 1.54184 |
| Radiation type | Cu K$_a$ | Cu K$_a$ | Cu K$_a$ | Cu K$_a$ |
| $Q_{min}$/° | 2.289 | 2.575 | 4.005 | 6.935 |
| $Q_{max}$/° | 77.699 | 77.775 | 80.339 | 77.534 |
| Measured Refl's. | 18325 | 17543 | 12928 | 4728 |
| Indep't Refl's | 4958 | 3816 | 4293 | 1900 |
| Refl's I≥2 $s$(I) | 3887 | 2958 | 4252 | 1518 |
| $R_{int}$ | 0.0678 | 0.0835 | 0.0350 | 0.0405 |
| Parameters | 469 | 381 | 401 | 167 |
| Restraints | 0 | 0 | 68 | 0 |
| Largest Peak | 0.474 | 0.318 | 0.544 | 1.160 |
| Deepest Hole | -0.365 | -0.274 | -0.607 | -0.337 |
| GooF | 1.012 | 1.029 | 1.174 | 1.075 |
| $wR_2$ (all data) | 0.1348 | 0.1244 | 0.2023 | 0.2246 |
| $wR_2$ | 0.1232 | 0.1138 | 0.2020 | 0.2102 |
| $R_1$ (all data) | 0.0658 | 0.0640 | 0.0892 | 0.0843 |
| $R_1$ | 0.0496 | 0.0473 | 0.0886 | 0.0730 |

**Table S2:** Crystallographic data for **ISEM-6, 9-TATOT**, **ISEM-3-$H_2O$** and **ISEM-6-$H_2O$.**

| **Compound** | **ISEM-6** | **9-TATOT** | **ISEM-3-$H_2O$** | **ISEM-6-$H_2O$** |
|---|---|---|---|---|
| CCDC # | 2350606 | 2345099 | 2346398 | 2350679 |
| Formula | $C_{20}H_{28}N_{44}O_{18}$ | $C_6H_8N_{15}O_{4.5}$ | $C_8H_{18}N_{24}O_6$ | $C_{10}H_{16}N_{22}O_{10}$ |
| $D_{calc.}$/ g cm$^{-3}$ | 1.855 | 1.771 | 1.759 | 1.792 |
| $m$/mm$^{-1}$ | 1.419 | 1.327 | 1.300 | 1.384 |
| Formula Weight | 1172.86 | 362.27 | 546.46 | 604.45 |
| Color | green | yellow | orange | yellow |
| Shape | needle-shaped | cube-shaped | plate-shaped | plate-shaped |
| Size/mm$^3$ | 0.18×0.03×0.02 | 0.20×0.15×0.03 | 0.13×0.07×0.02 | 0.15×0.09×0.03 |
| $T$/K | 99.99(10) | 99.98(10) | 100.00(10) | 100.01(10) |
| Crystal System | orthorhombic | orthorhombic | triclinic | orthorhombic |
| Flack Parameter | 0.6(5) | - | - | -0.03(19) |
| Hooft Parameter | -0.1(3) | - | - | 0.06(15) |
| Space Group | $Pca2_1$ | $Pbcn$ | $P$-1 | $Pna2_1$ |
| $a$/Å | 20.2501(8) | 21.7598(3) | 7.48693(15) | 8.30682(19) |
| $b$/Å | 5.35469(14) | 6.30828(8) | 11.5802(2) | 52.5690(11) |
| $c$/Å | 38.7326(8) | 19.7952(2) | 12.4606(2) | 5.13161(17) |
| $\alpha$/° | 90 | 90 | 104.8425(15) | 90 |
| $\beta$/° | 90 | 90 | 90.1568(15) | 90 |
| $\gamma$/° | 90 | 90 | 98.5391(17) | 90 |
| V/Å$^3$ | 4199.9(2) | 2717.24(6) | 1031.77(3) | 2240.88(10) |
| $Z$ | 4 | 8 | 2 | 4 |
| $Z'$ | 1 | 1 | 1 | 1 |
| Wavelength/Å | 1.54184 | 1.54184 | 1.54184 | 1.54184 |
| Radiation type | Cu $K_a$ | Cu $K_a$ | Cu $K_a$ | Cu $K_a$ |
| $Q_{min}$/° | 4.367 | 4.063 | 3.673 | 3.363 |
| $Q_{max}$/° | 80.098 | 77.047 | 80.325 | 80.271 |
| Measured Refl's. | 25412 | 10610 | 14362 | 40579 |
| Indep't Refl's | 6968 | 2744 | 4394 | 4905 |
| Refl's I≥2 $s$(I) | 5732 | 2507 | 3613 | 4465 |
| $R_{int}$ | 0.0879 | 0.0358 | 0.0346 | 0.0989 |
| Parameters | 744 | 263 | 424 | 443 |
| Restraints | 1 | 0 | 0 | 1 |
| Largest Peak | 0.483 | 0.297 | 0.247 | 0.328 |
| Deepest Hole | -0.334 | -0.330 | -0.261 | -0.259 |
| GooF | 1.033 | 1.162 | 1.057 | 1.077 |
| $wR_2$ (all data) | 0.1310 | 0.1044 | 0.1015 | 0.1115 |
| $wR_2$ | 0.1233 | 0.0990 | 0.0960 | 0.1075 |
| $R_1$ (all data) | 0.0734 | 0.0428 | 0.0461 | 0.0480 |
| $R_1$ | 0.0571 | 0.0394 | 0.0368 | 0.0429 |

**Section S3 Enthalpy of formation**

**Section S3.1. Isodesmic reactions**

The $\Delta H_f$ (Enthalpy of formation) for **ISEM-1**[9], and **ISEM-5**[6] are obtained from literature.

The $\Delta H_f$ (Enthalpy of formation) for the anions corresponding to **2**, **3**, **4**, **6**, **7**, and **8** were calculated by using isodesmic reactions (Scheme S1).

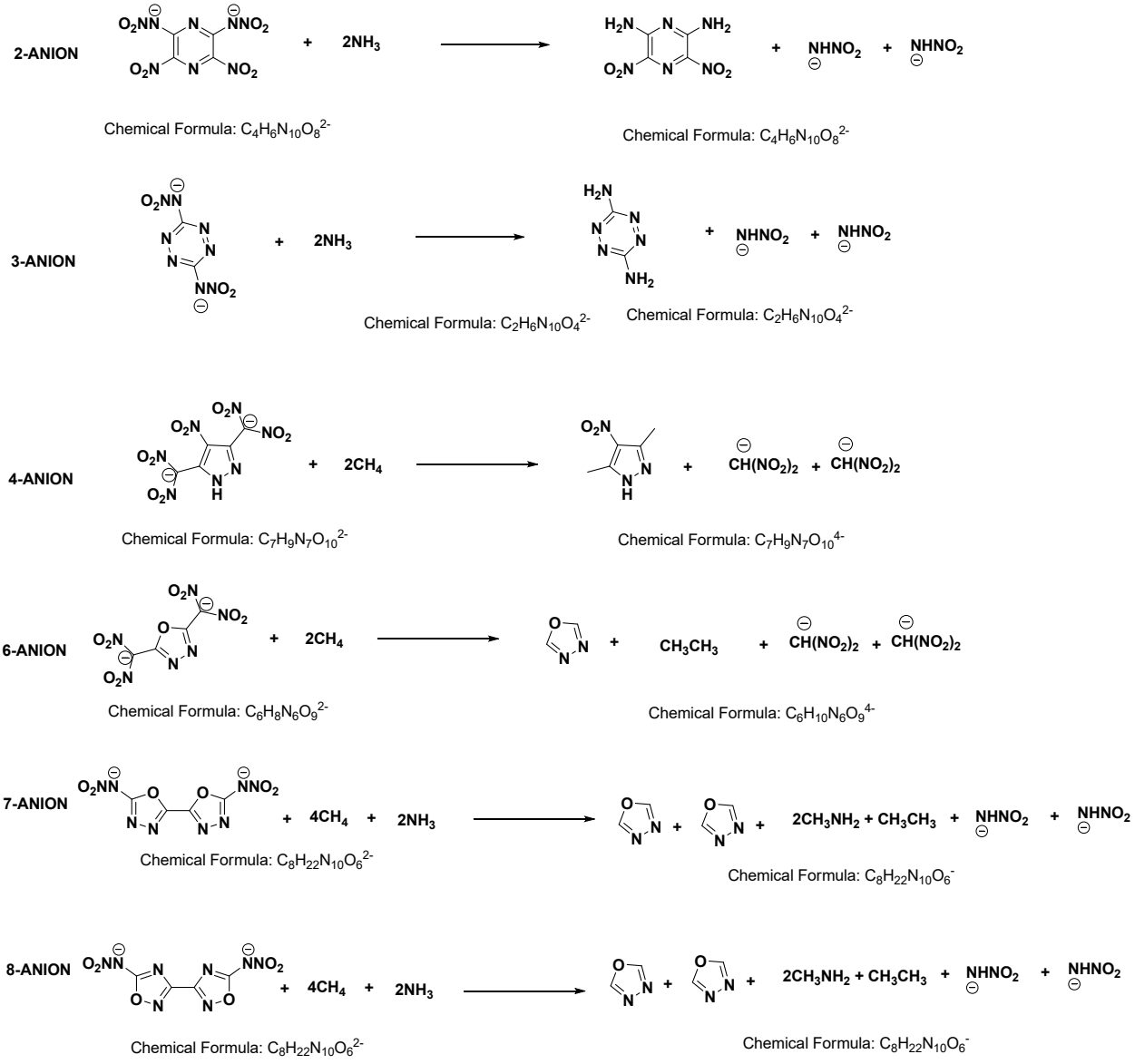


**Scheme S1**: Isodesmic reactions.

The single crystal structure was used for the geometric optimization and frequency analyses using the B3LYP functional with the 6-31+G** basis set. The single-point energies were obtained at the MP2/6-

311++G** level (Table S8).[14] The atomization energies for cations were calculated by using the G[2]*ab initio* method [15] All of the optimized structures were characterized to be true local energy minima on the potential energy surface without imaginary frequencies. In case of the energetic salts, the solid-phase heats of formation were obtained based on a Born–Haber energy cycle.[16] All calculated gas-phase enthalpies for covalent materials are converted to solid phase values by subtracting the empirical heat of sublimation obtained based on Trouton's rule.[17,18,19, 20]

**Section S4. References**


1. J. Singh, A. K. Chinnam, R. J. Staples and J. M. Shreeve, *Inorg. Chem.*, 2022, **61**, 16493–16500.

2. H. Li, T. Zhang, Z. Li, Y. Wang, J. Ren and T. Zhang, *J. Energ. Mater.*, 2022, **40**, 15–33.

3. J. Singh, R. J. Staples and J. M. Shreeve, *ACS Appl. Mater. Interfaces*, 2021, **13**, 61357–61364.

4. M. M. Williams, W. S. Mcewan and R. A. Henry, *J. Phys. Chem.*, 1957, **61**, 261–267.

5. Q. Yu, P. Yin, J. Zhang, C. He, G. H. Imler, D. A. Parrish and J. M. Shreeve, *J. Am. Chem. Soc.*, 2017, **139**, 8816–8819.

6. T. S. Hermann, K. Karaghiosoff, T. M. Klapötke, J. Stierstorfer, *Chem. Eur. J.* **2017**, *23*, 12087.

7. Y. Cao, H. Huang, X. Lin, J. Yang and X. Gong, *New J. Chem.*, 2018, **42**, 11390–11395.

8. X. Y. Zhang, X. Y. Lin, B. Y. Guo, C. Tan and Y. Han, *J. Mol. Struct.*, 2022, **1267**, 133526.

9. J. Singh, S. Lal, R. J. Staples and J. M. Shreeve, *Mater. Chem. Front.*, 2022, **6**, 933–938.

11. G. M. Sheldrick, *Acta Crystallogr. Sect. A Found. Crystallogr.* 2008, **64**, 112–122.

12. G. M. Sheldrick, *Acta Crystallogr. Sect. A Found. Adv.* 2015, **71**, 3–8.

13. O. V. Dolomanov, L. J. Bourhis, R. J. Gildea, J. A. K. Howard, H. Puschmann, *J. Appl. Crystallogr.* 2009, **42**, 339–341.

14. R. G. Parr, Y. Weitao, *Density-Functional Theory of Atoms and Molecules* (Oxford University Press, 1995).

15. O. Suleimenov, T.-K. Ha, *Chem. Phys. Lett.* 1998, **290**, 451–457.

16. H. D. B. Jenkins, D. Tudela, L. Glasser, *Inorg. Chem.* 2002, **41**, 2364–2367.

17. M. S. Westwell, M. S. Searle, D. J. Wales, D. H. Williams, *J. Am. Chem. Soc.* 1995, **117**, 5013–5015.

18. S. Wahler, P. Chung, T. M. Klapötke, *J. Energ. Mater.* 2023, doi:10.1080/07370652.2023.2219678.

19. N. V. Muravyev, K. A. Monogarov, I. N. Melnikov, A. N. Pivkina, V. G. Kiselev, *Phys. Chem. Chem. Phys.* 2021, **23**, 15522–15542.

20. A. L. R. Silva, A. R. R. P. Almeida, M. D. M. C. Ribeiro da Silva, J. Reinhardt and T. M. Klapötke, *Propellants, Explos. Pyrotech.*, 2023, **48**, e202200361.

## Section S5. Spectra Analysis

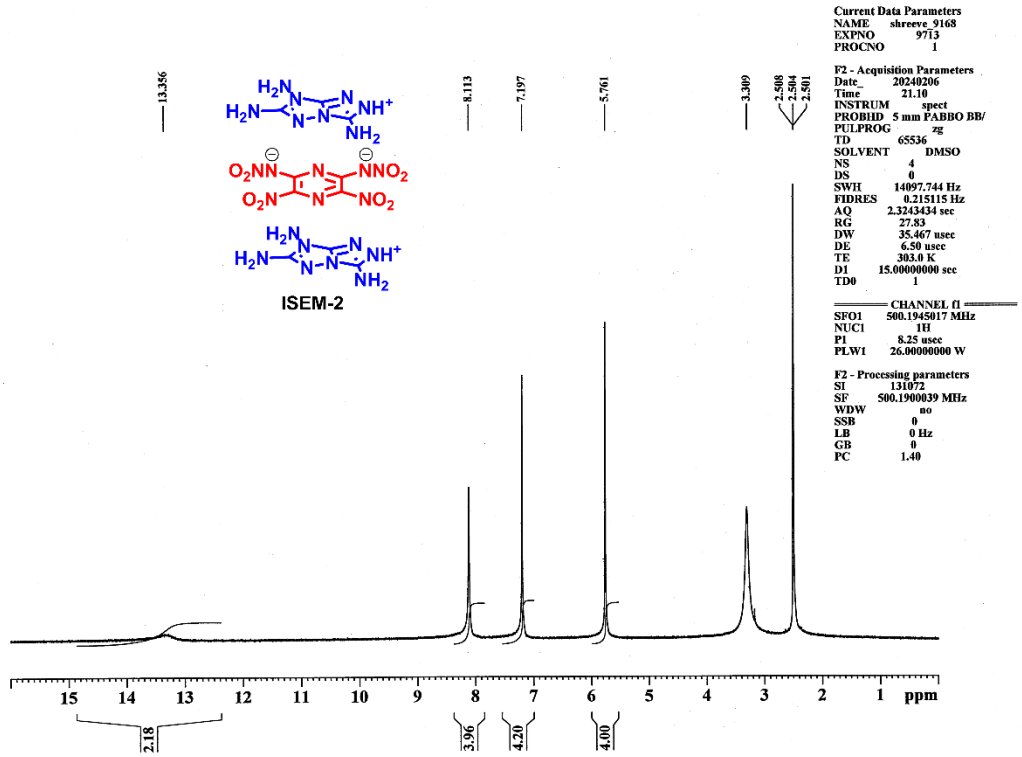


**Figure S9**: [1]H NMR spectrum of **ISEM-2**.

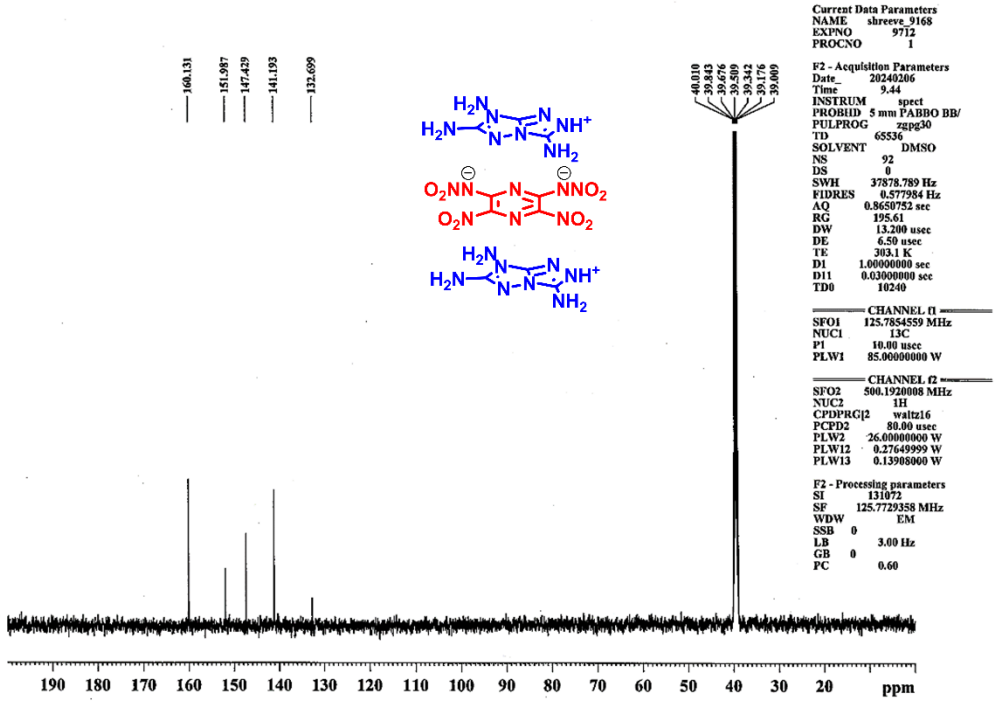

**Figure S10**: $^{13}C$ NMR spectrum of **ISEM-2**.

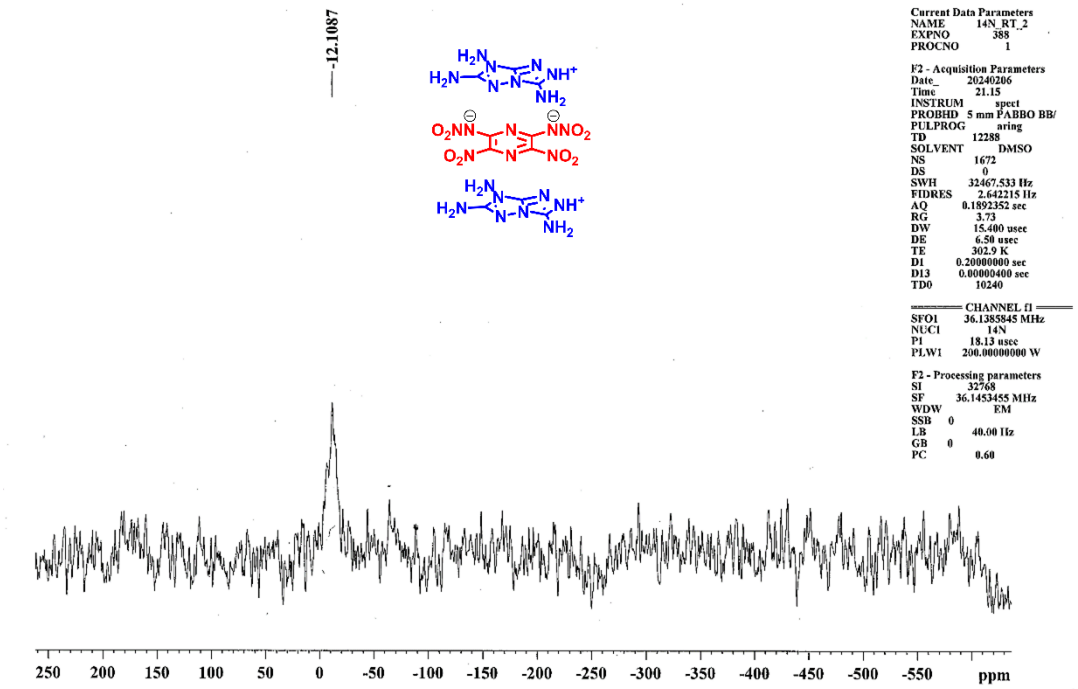


**Figure S11**: $^{14}N$ NMR spectrum of compound **ISEM-2**.

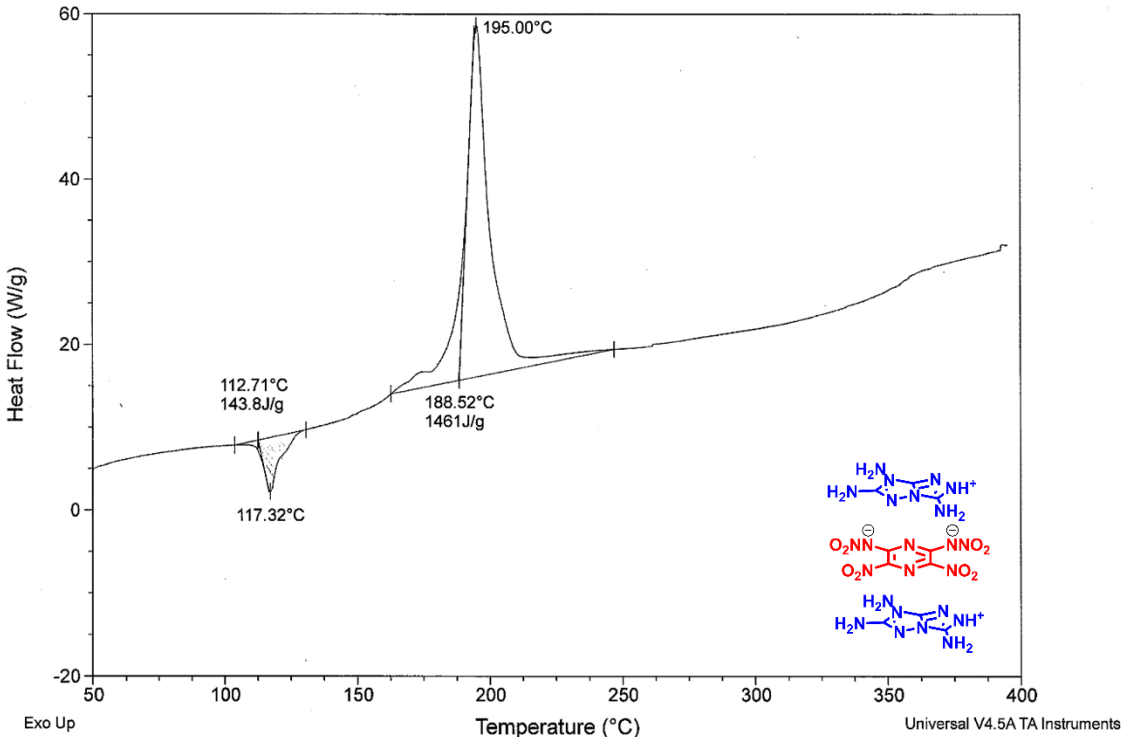


**Figure S12**: DSC plot for **ISEM-2** at the heating rate of 5 °C/min.

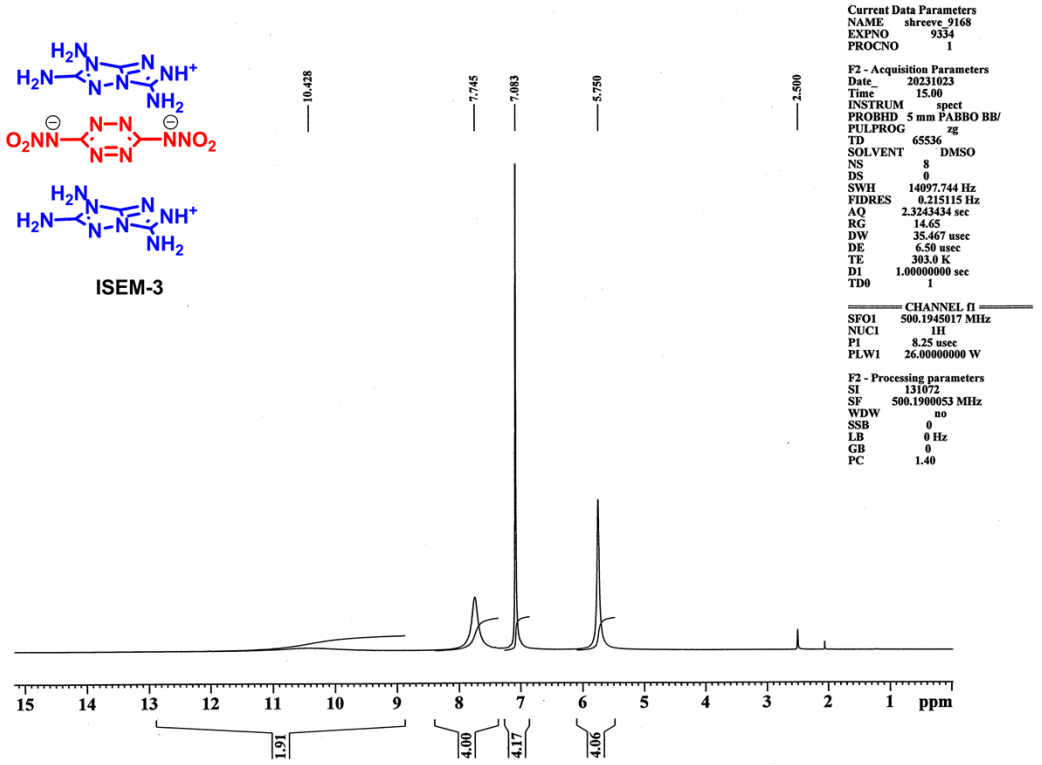


**Figure S13**: [1]H NMR spectrum of **ISEM-3**.

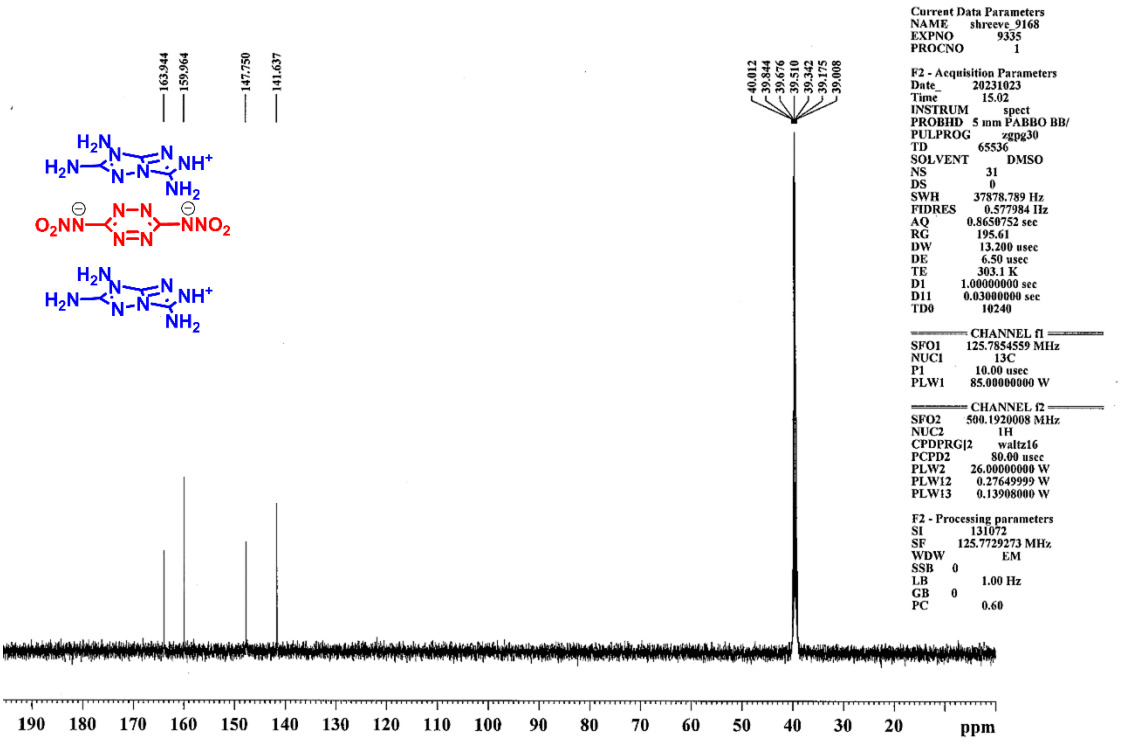


**Figure S14**: [13]C NMR spectrum of **ISEM-3**.

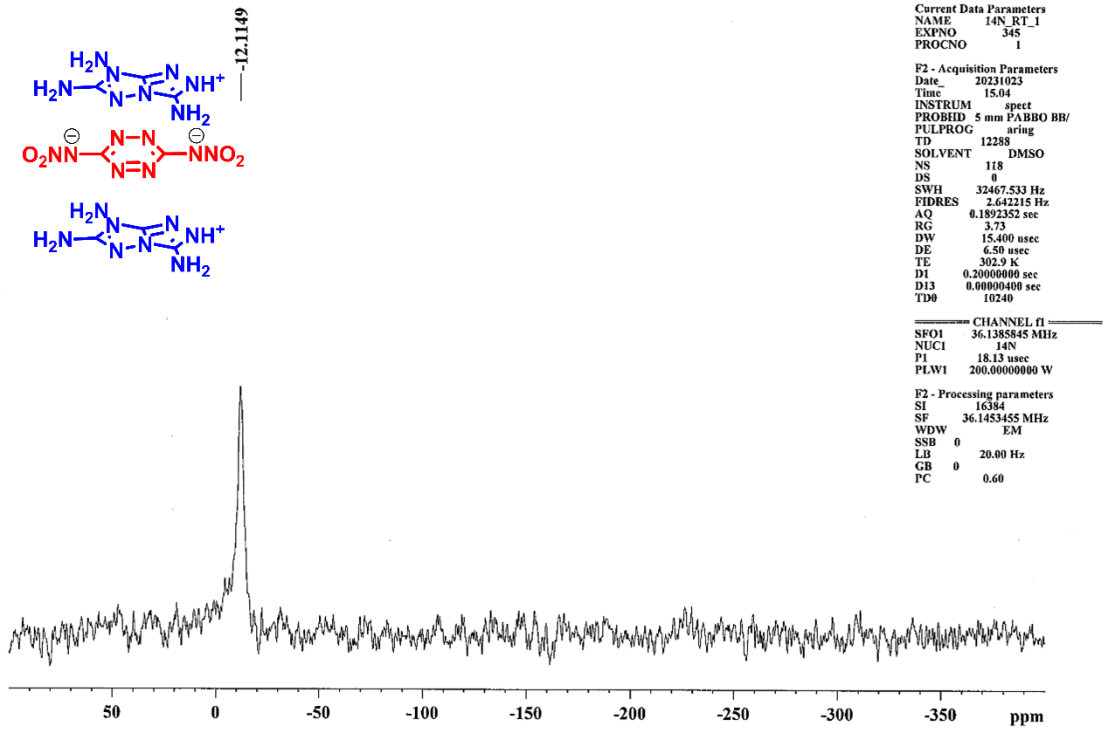


**Figure S15**: $^{14}$N NMR spectrum of compound **ISEM-3**.

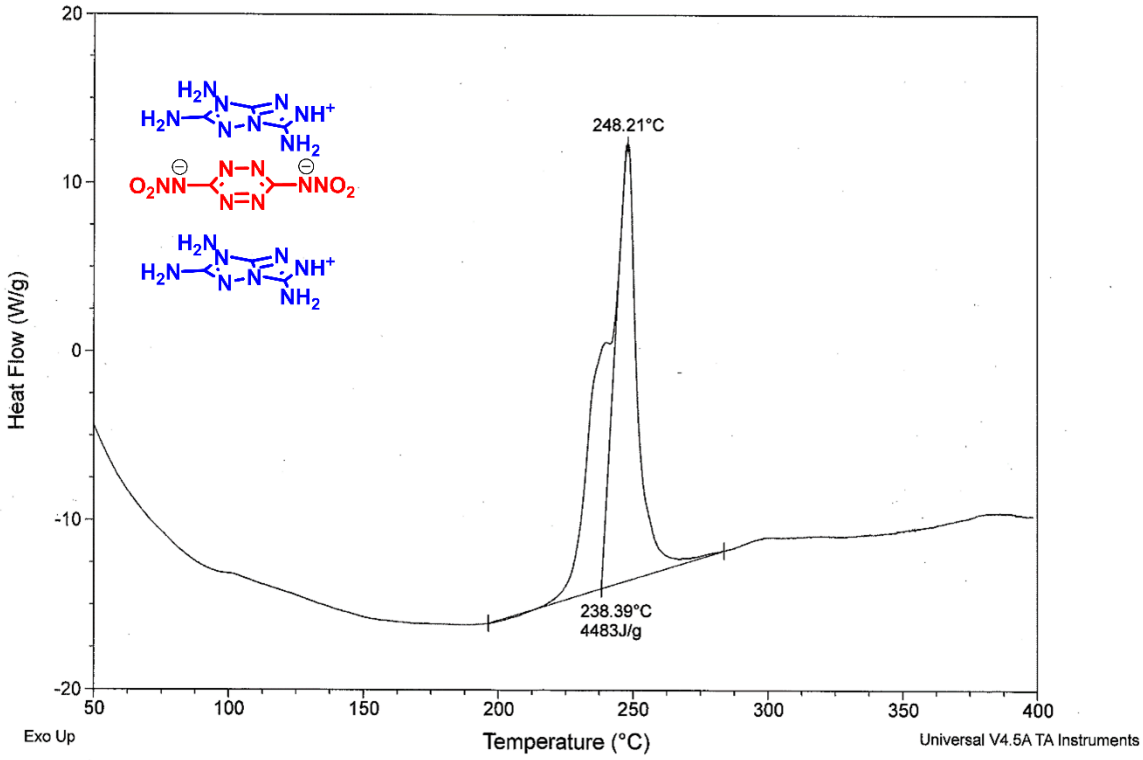


**Figure S16**: DSC plot for **ISEM-3** at the heating rate of 5 °C/min.

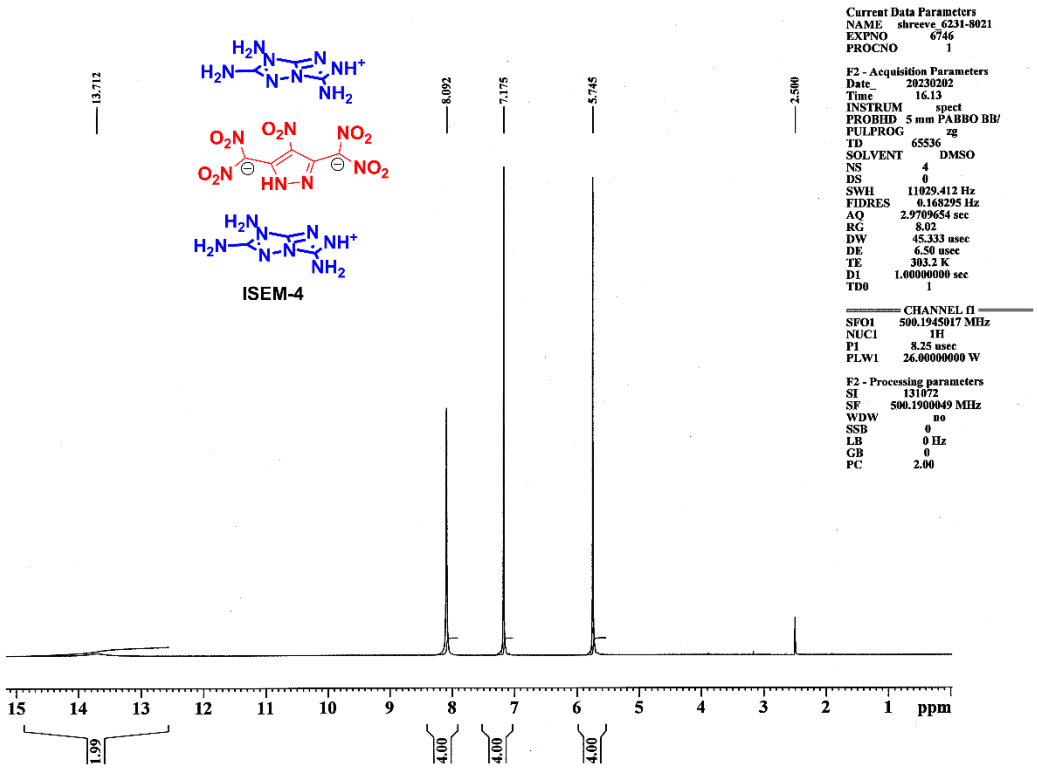


**Figure S17**: [1]H NMR spectrum of **ISEM-4**.

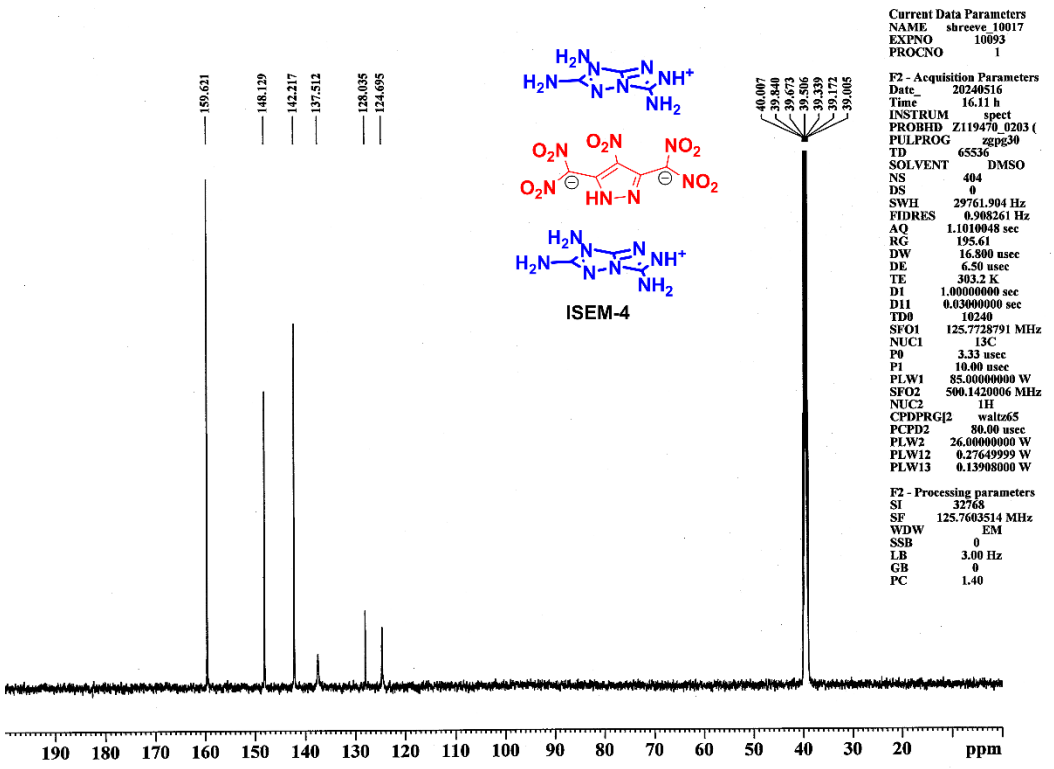


**Figure S18**: [13]C NMR spectrum of **ISEM-4**.

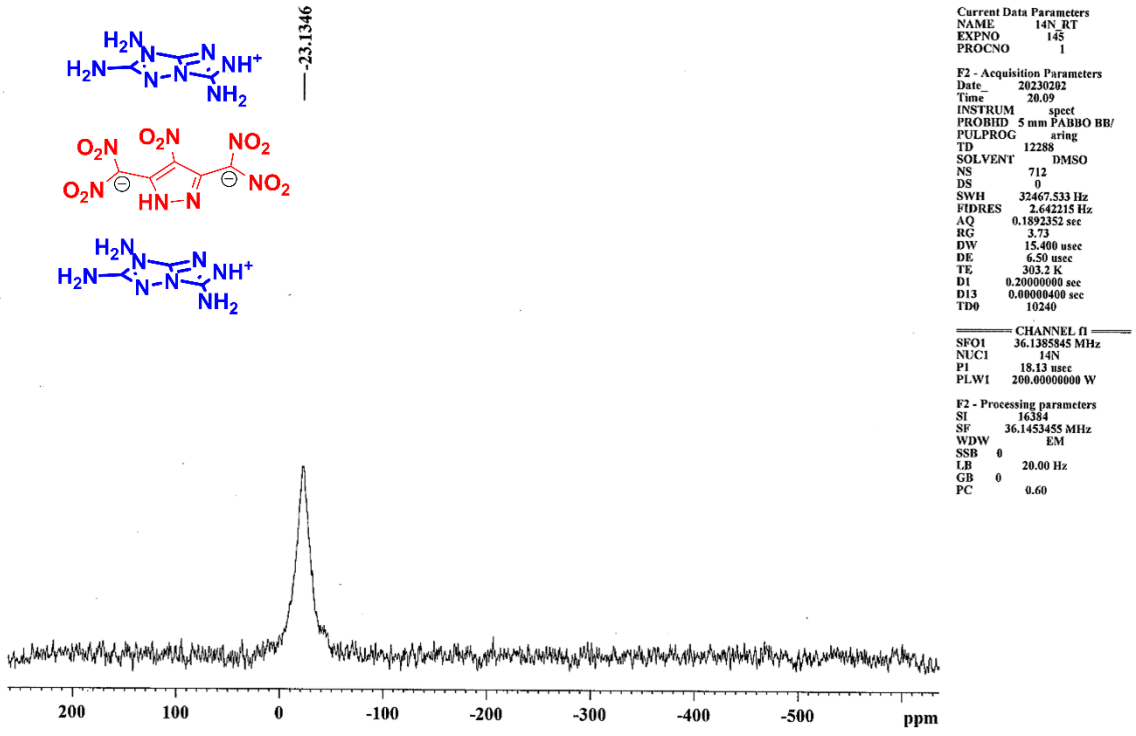


**Figure S19**: $^{14}$N NMR spectrum of compound **ISEM-4**.

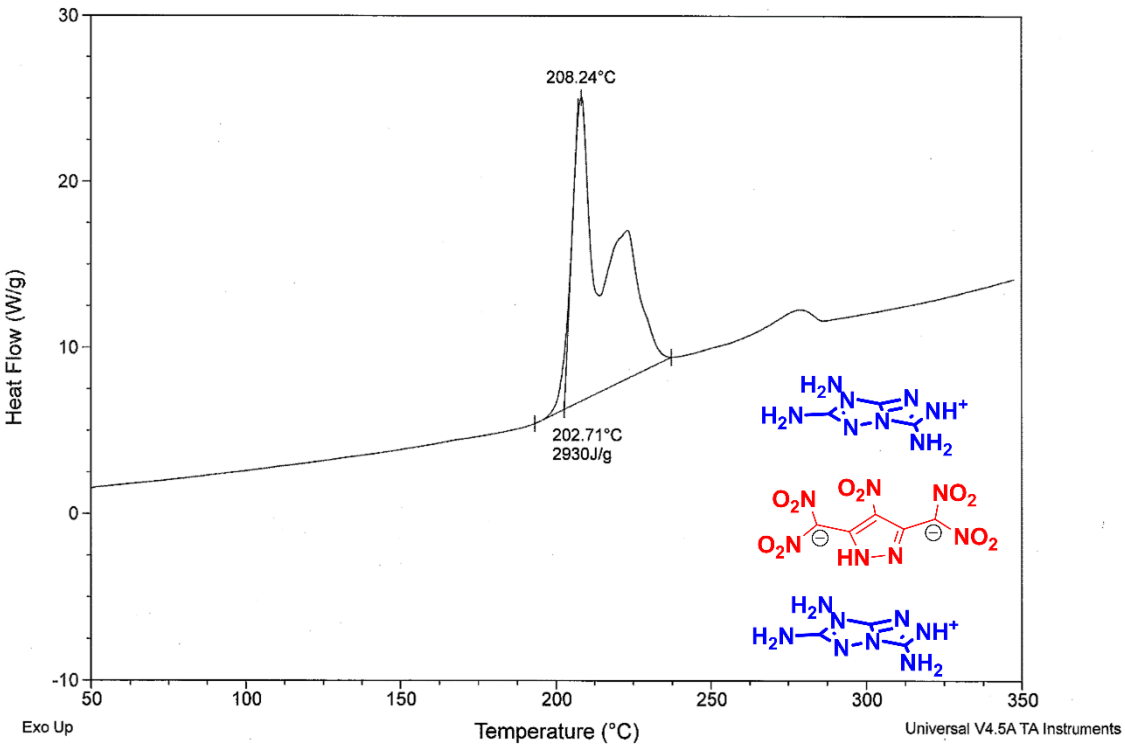


**Figure S20**: DSC plot for **ISEM-4** at the heating rate of 5 °C/min.

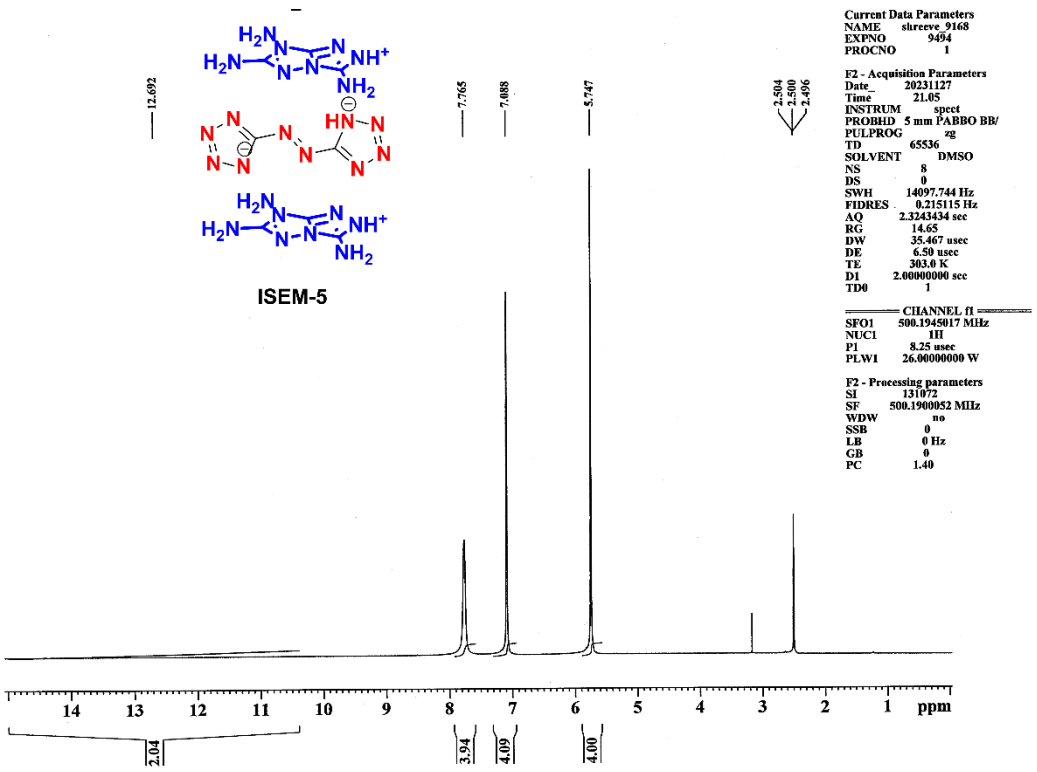


**Figure S21**: [1]H NMR spectrum of **ISEM-5**.

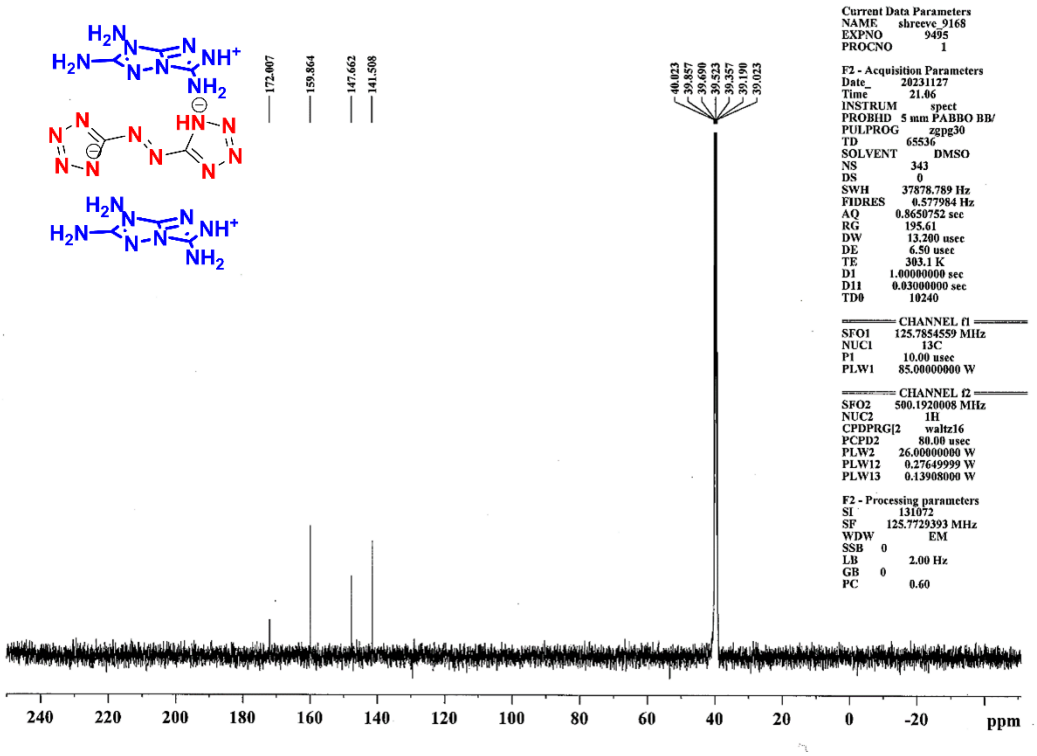


**Figure S22**: [13]C NMR spectrum of **ISEM-5**.

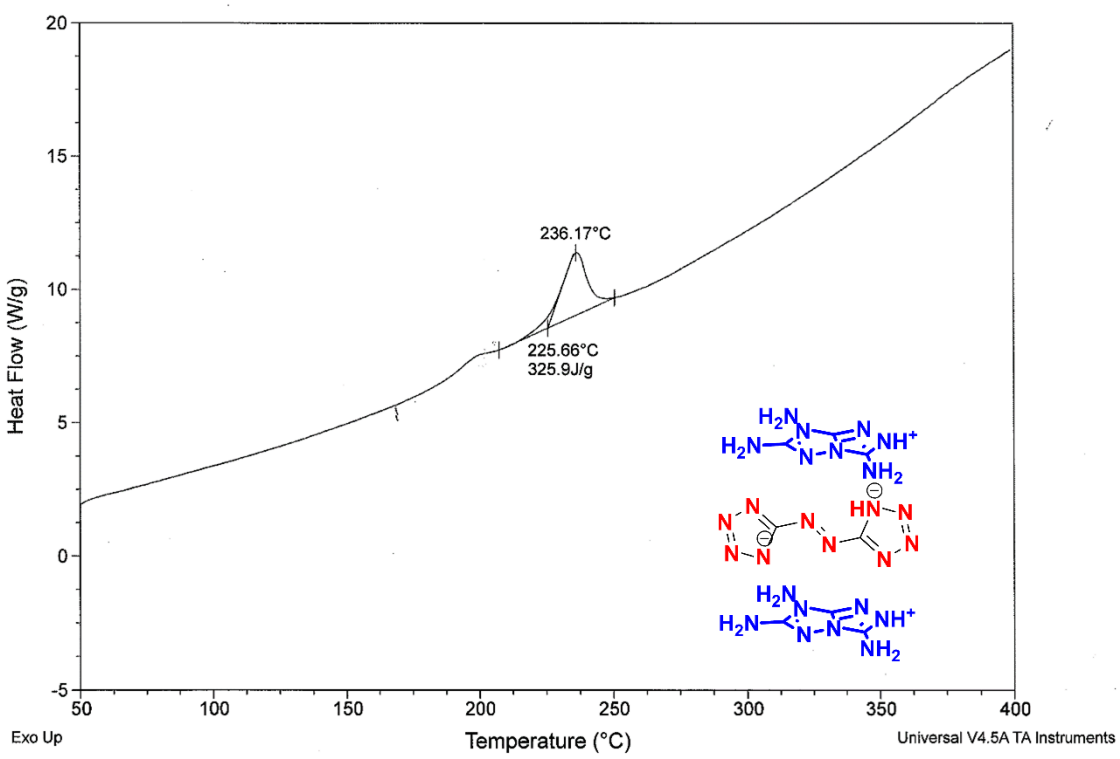


**Figure S23**: DSC plot for **ISEM-5** at the heating rate of 5 °C/min.

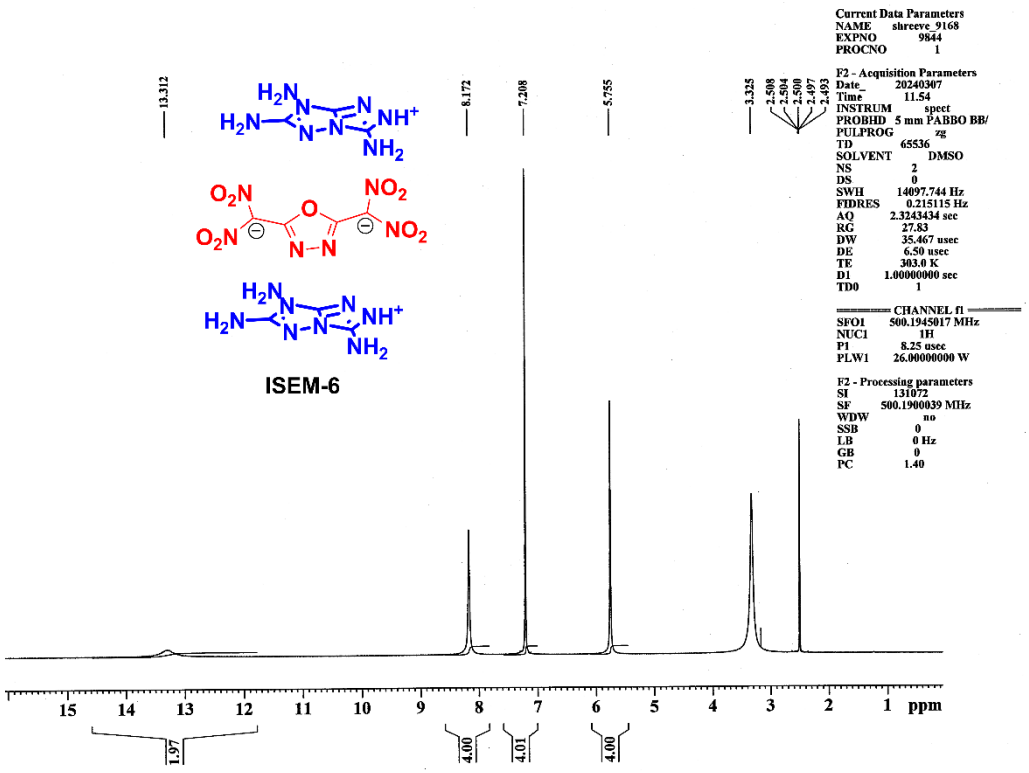


**Figure S24**: $^{1}$H NMR spectrum of **ISEM-6**.

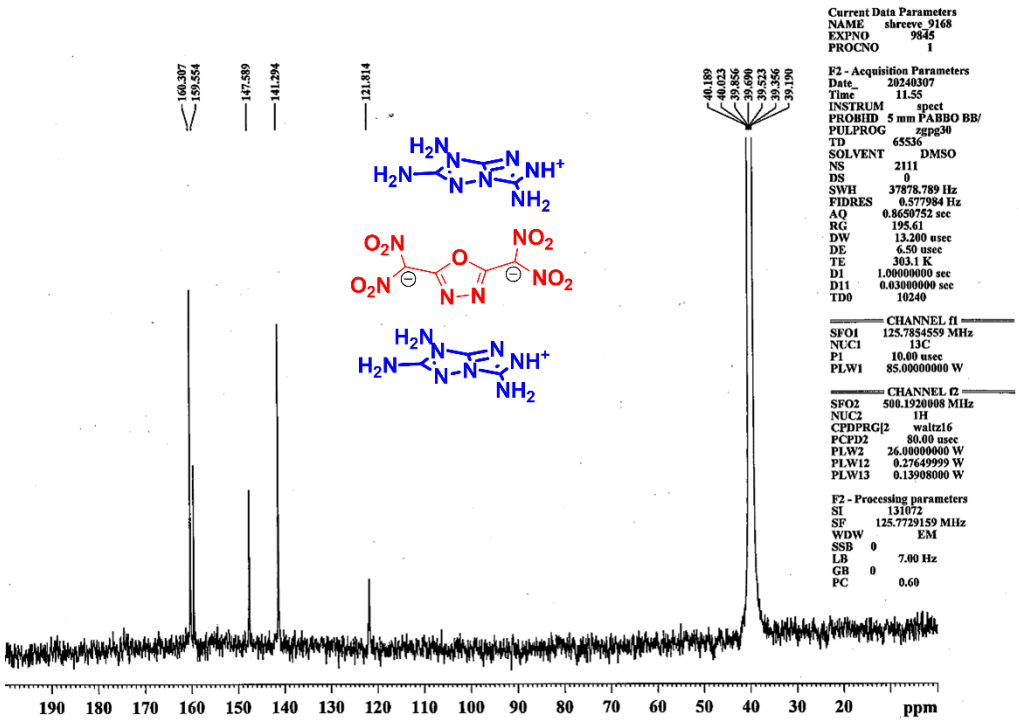


**Figure S25**: $^{13}C$ NMR spectrum of **ISEM-6**.

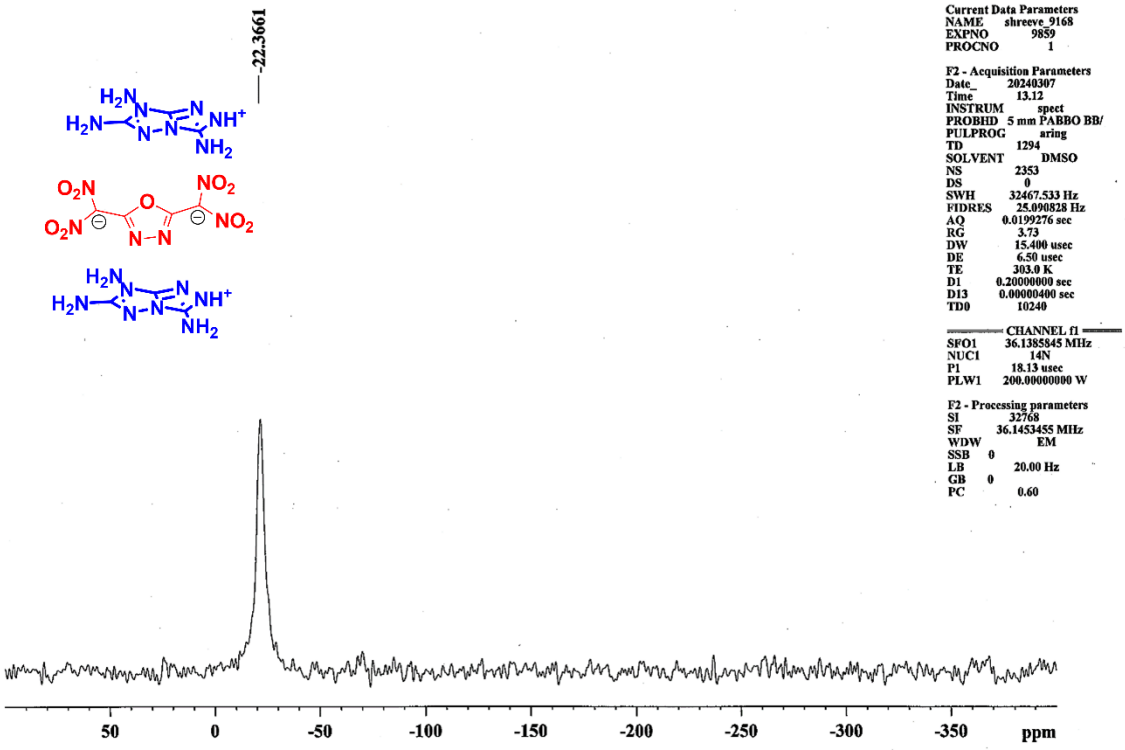


**Figure S26**: $^{14}N$ NMR spectrum of compound **ISEM-6**.

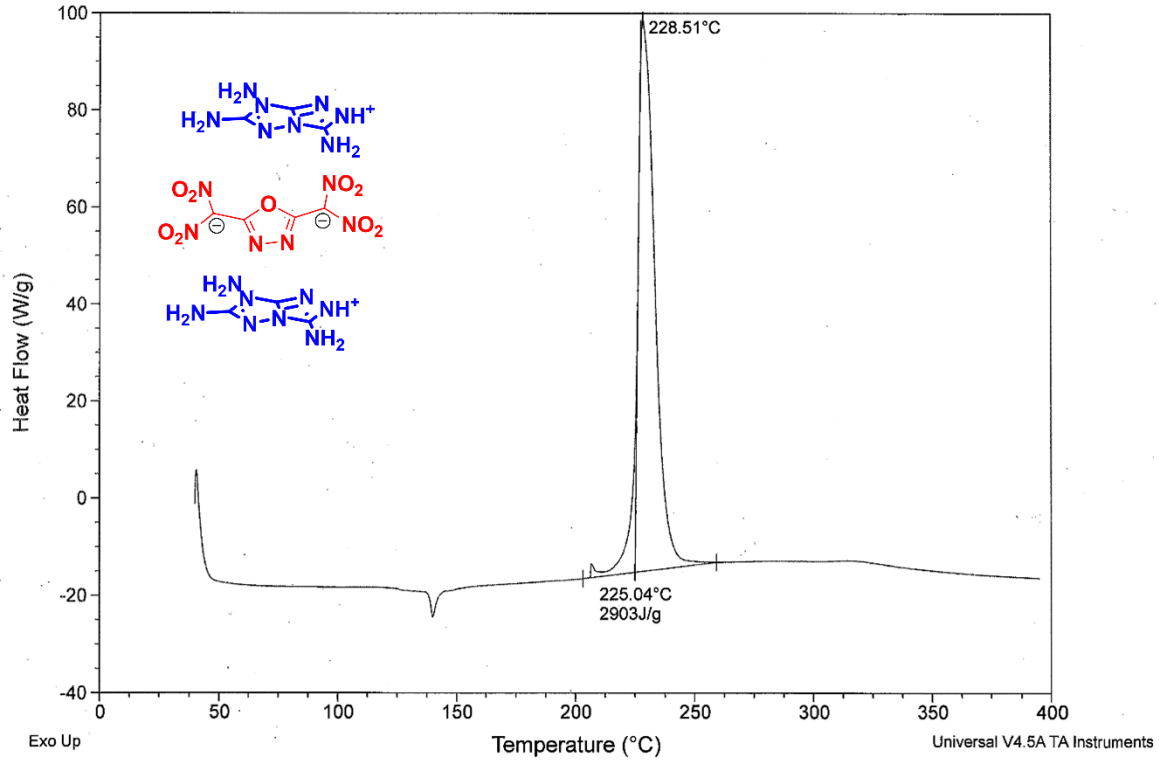


**Figure S27**: DSC plot for **ISEM-6** at the heating rate of 5 °C/min.

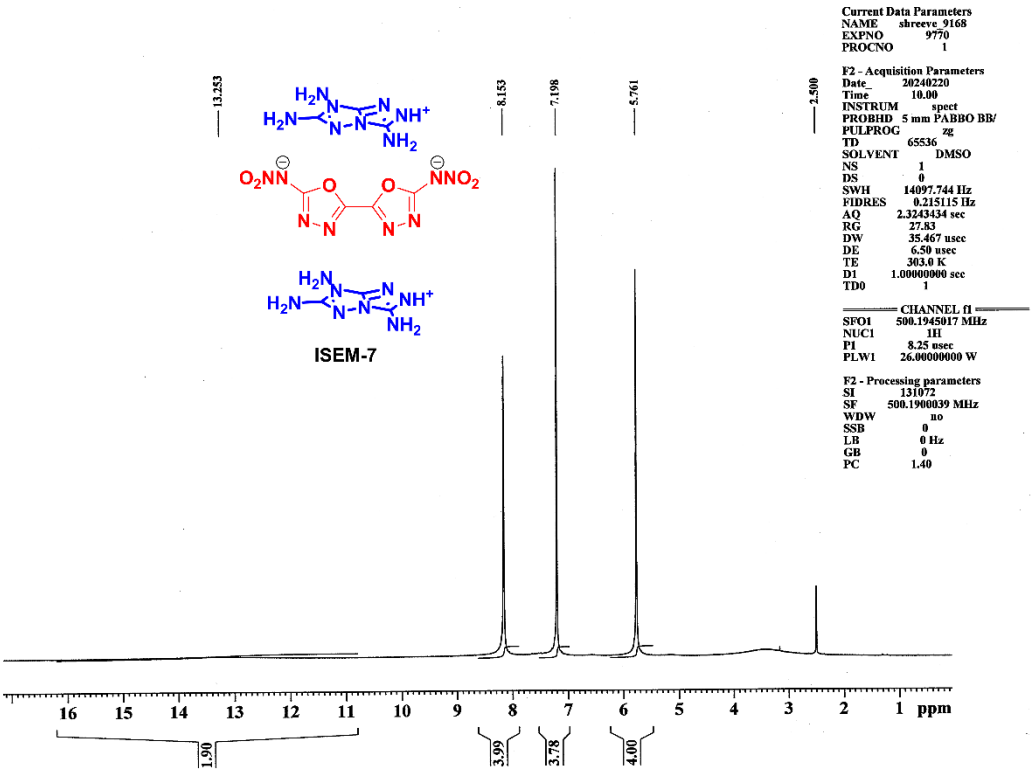


**Figure S28**: $^{1}$H NMR spectrum of **ISEM-7**.

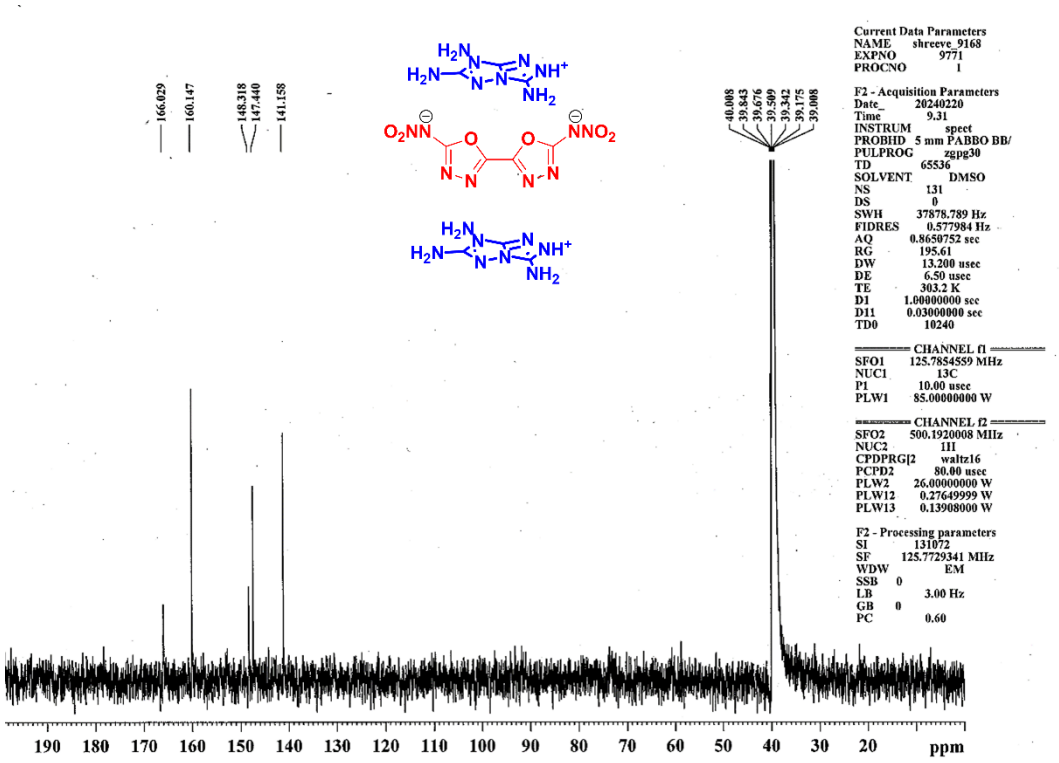


**Figure S29**: $^{13}$C NMR spectrum of **ISEM-7**.

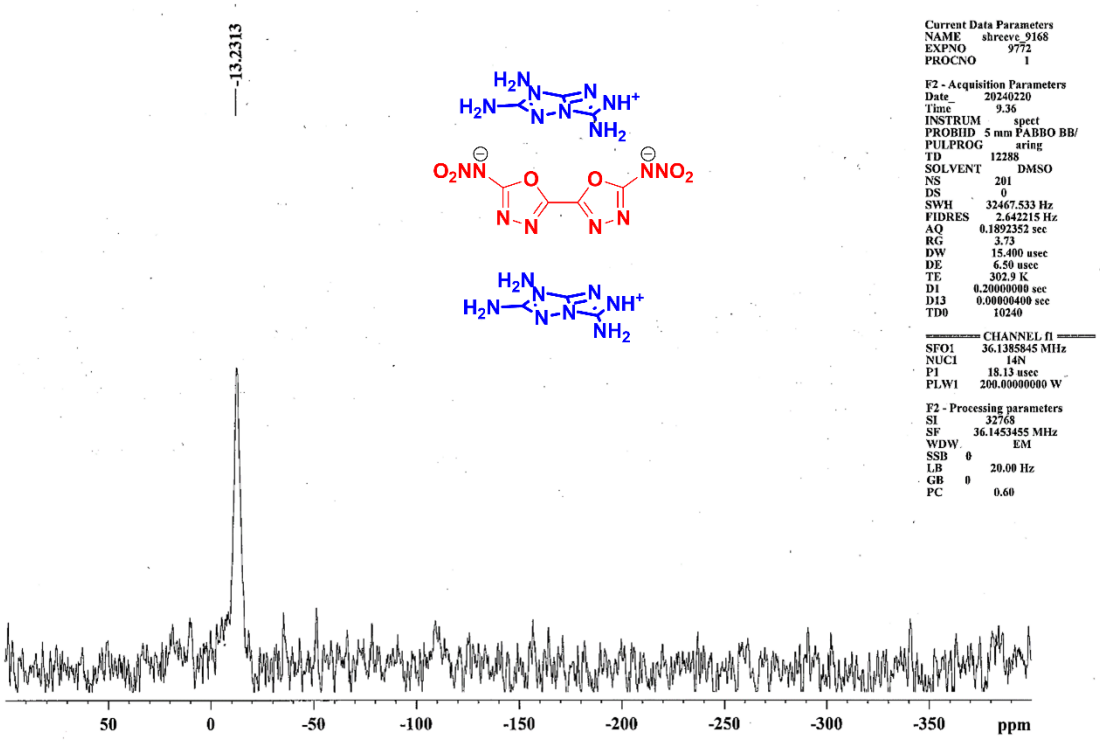


**Figure S30**: $^{14}$N NMR spectrum of compound **ISEM-7**.

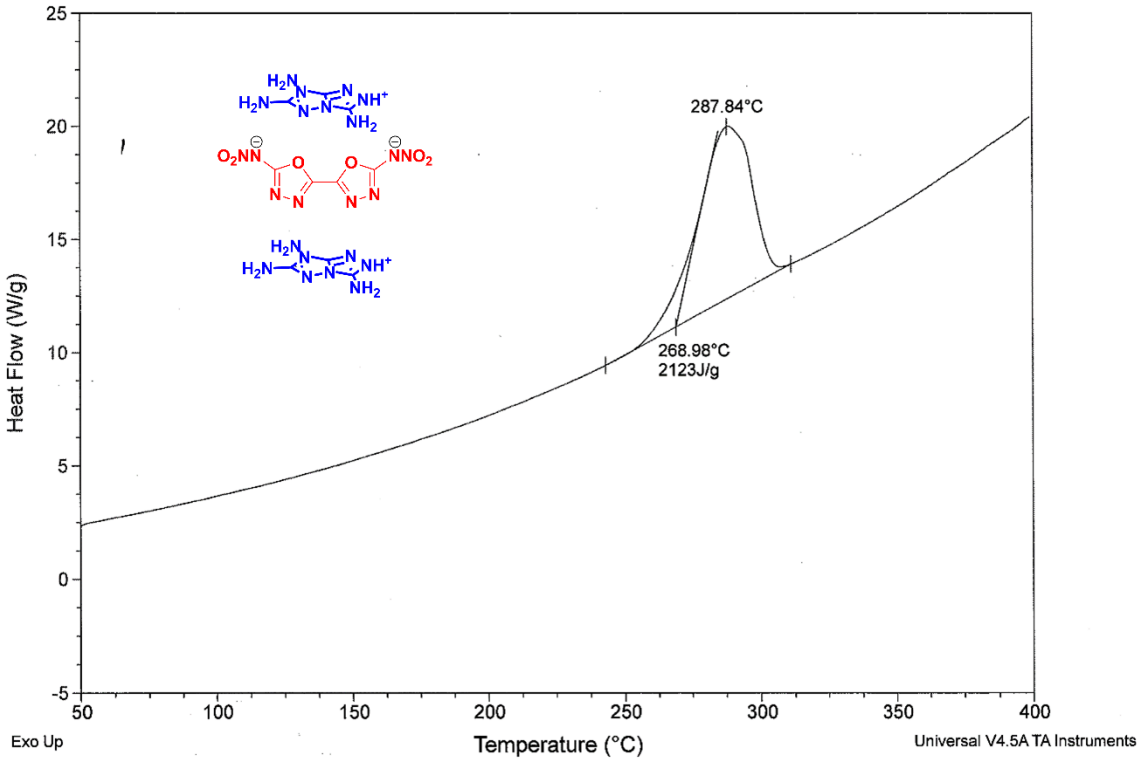


**Figure S31**: DSC plot for **ISEM-7** at the heating rate of 5 °C/min.

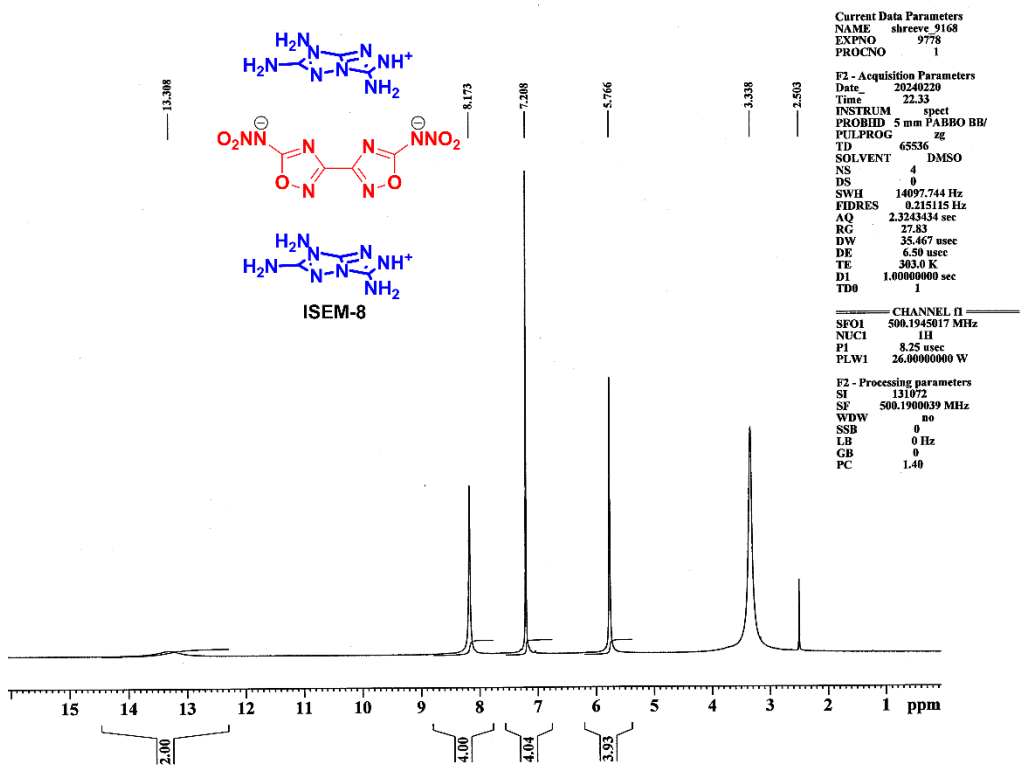


**Figure S32**: $^{1}$H NMR spectrum of **ISEM-8**.

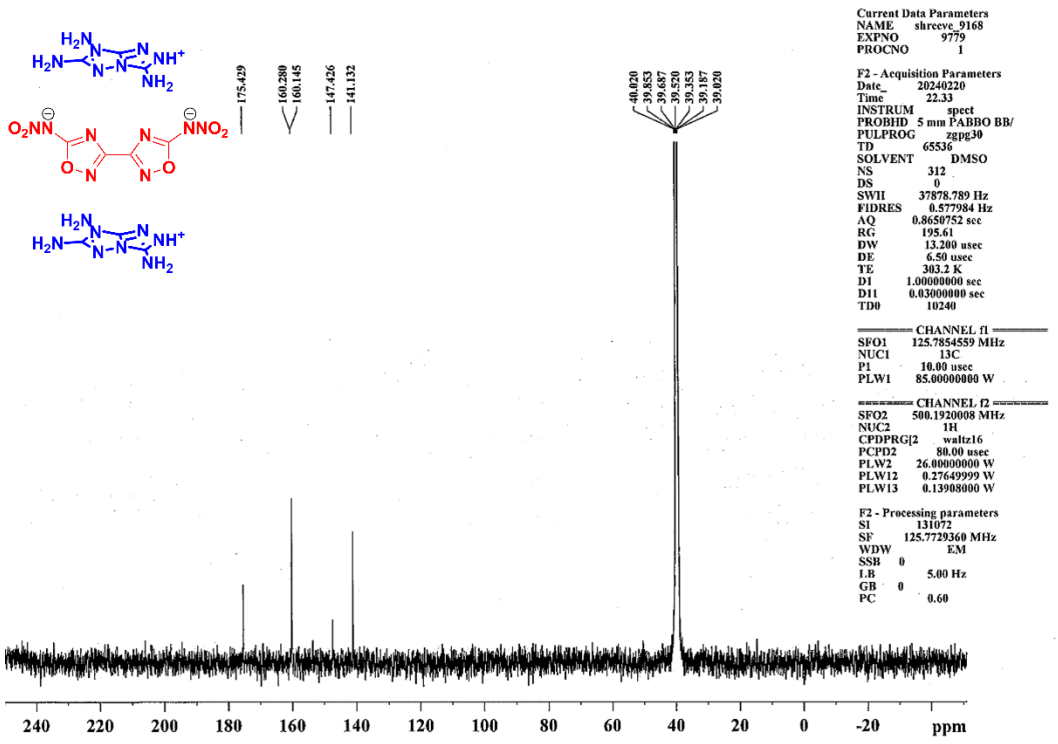


**Figure S33**: $^{13}$C NMR spectrum of **ISEM-8**

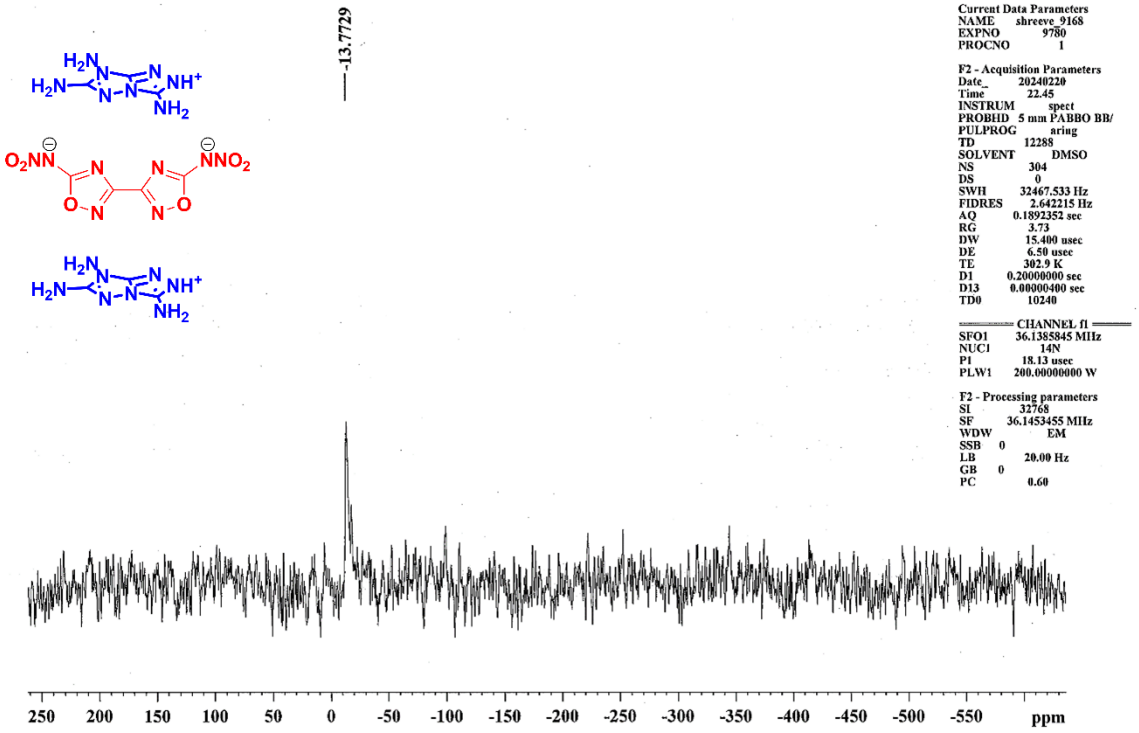


**Figure S34**: $^{14}$N NMR spectrum of compound **ISEM-8**.

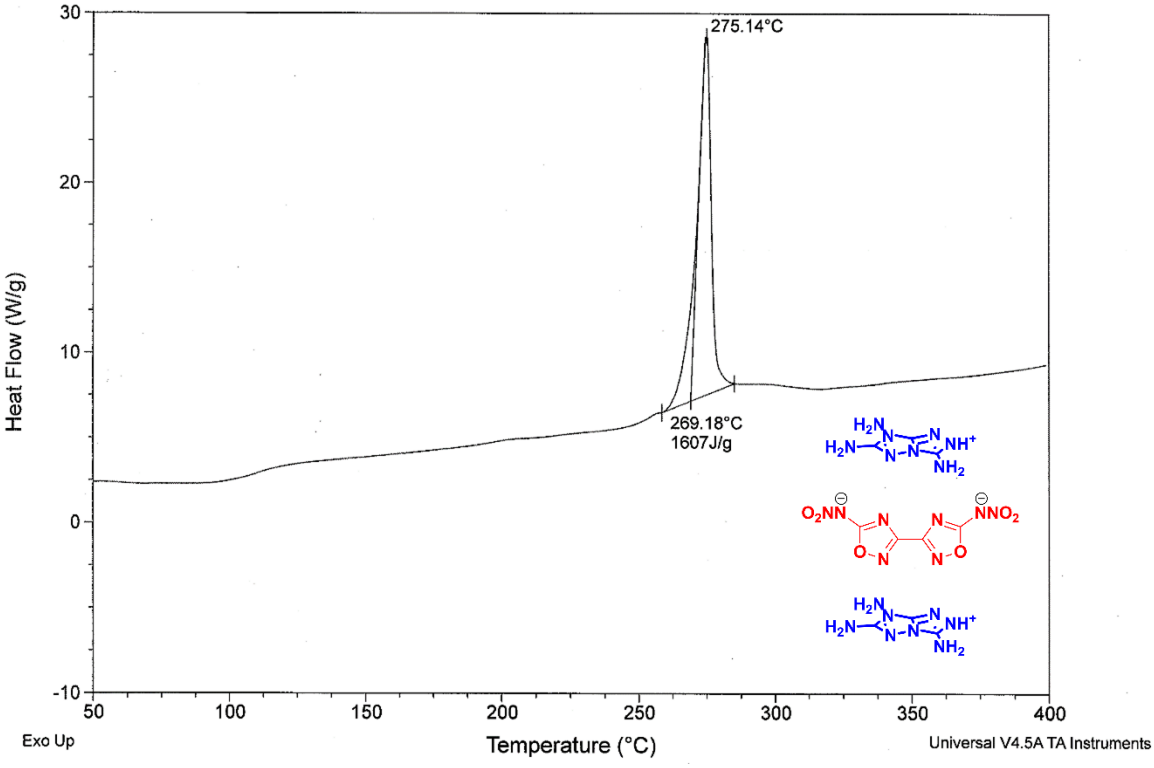


**Figure S35**: DSC plot for **ISEM-8** at the heating rate of 5 °C/min.

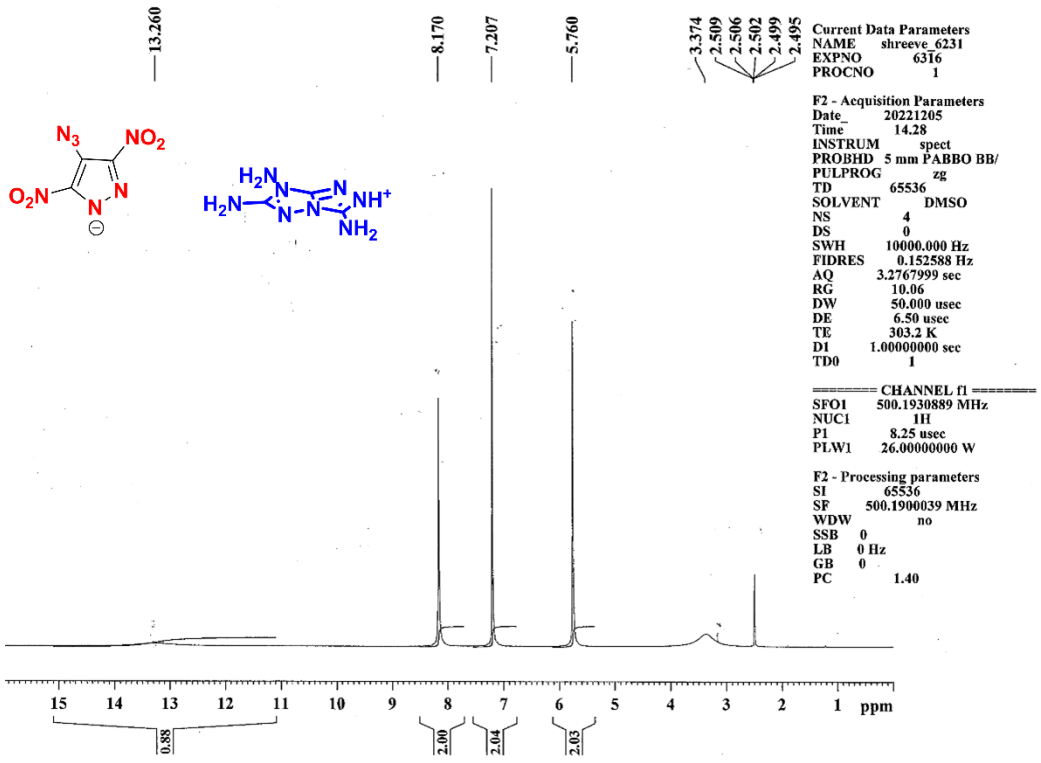


**Figure S36**: $^{1}$H NMR spectrum of **9-TATOT**.

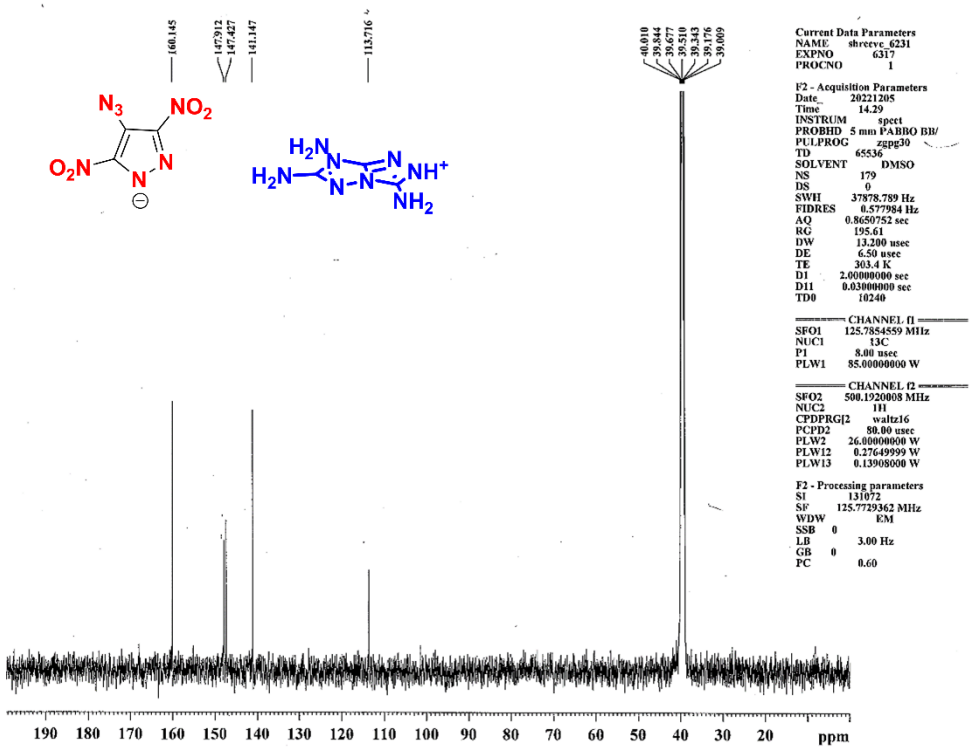


**Figure S37**: $^{13}$C NMR spectrum of **9-TATOT**.

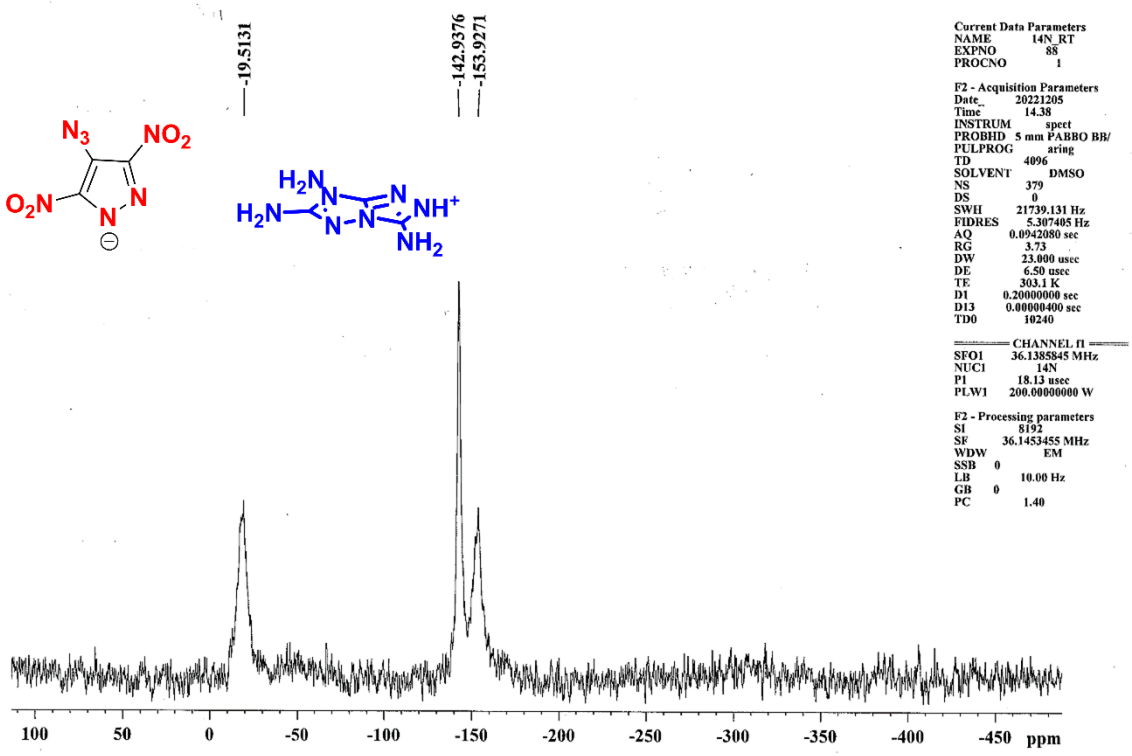


**Figure S38**: $^{14}$N NMR spectrum of compound **9-TATOT**.

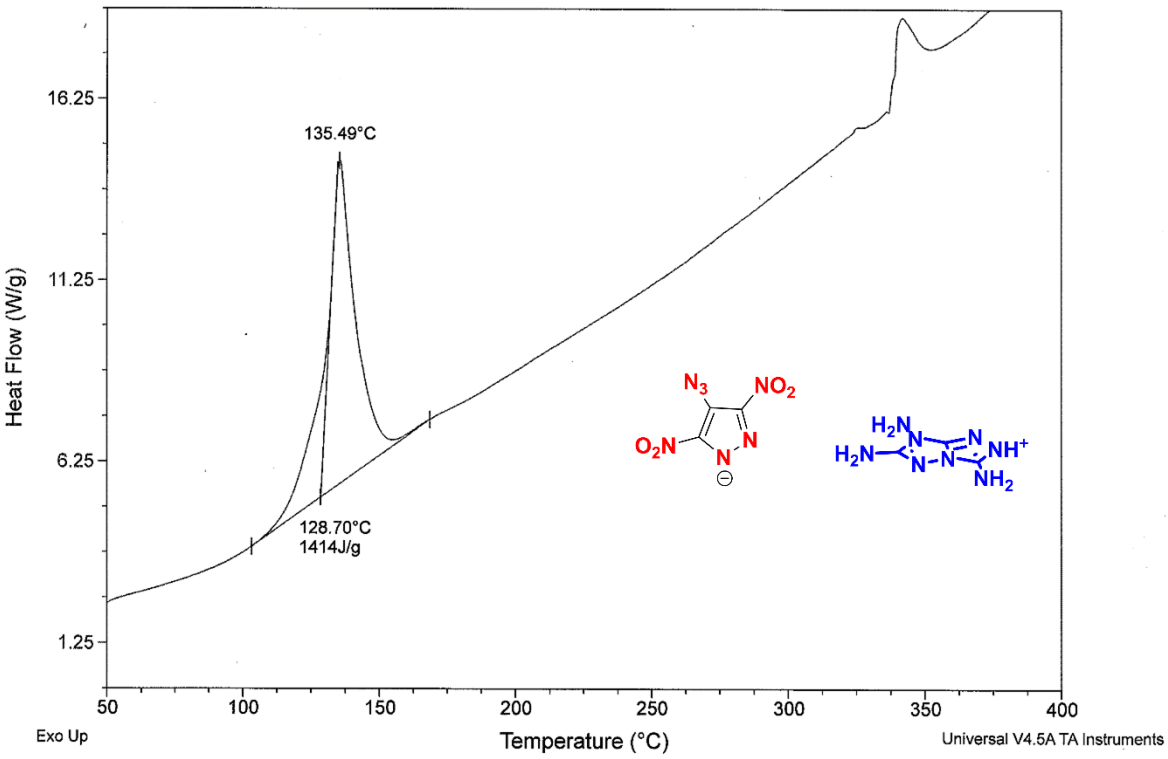


**Figure S39**: DSC plot for **9-TATOT** at the heating rate of 5 °C/min.

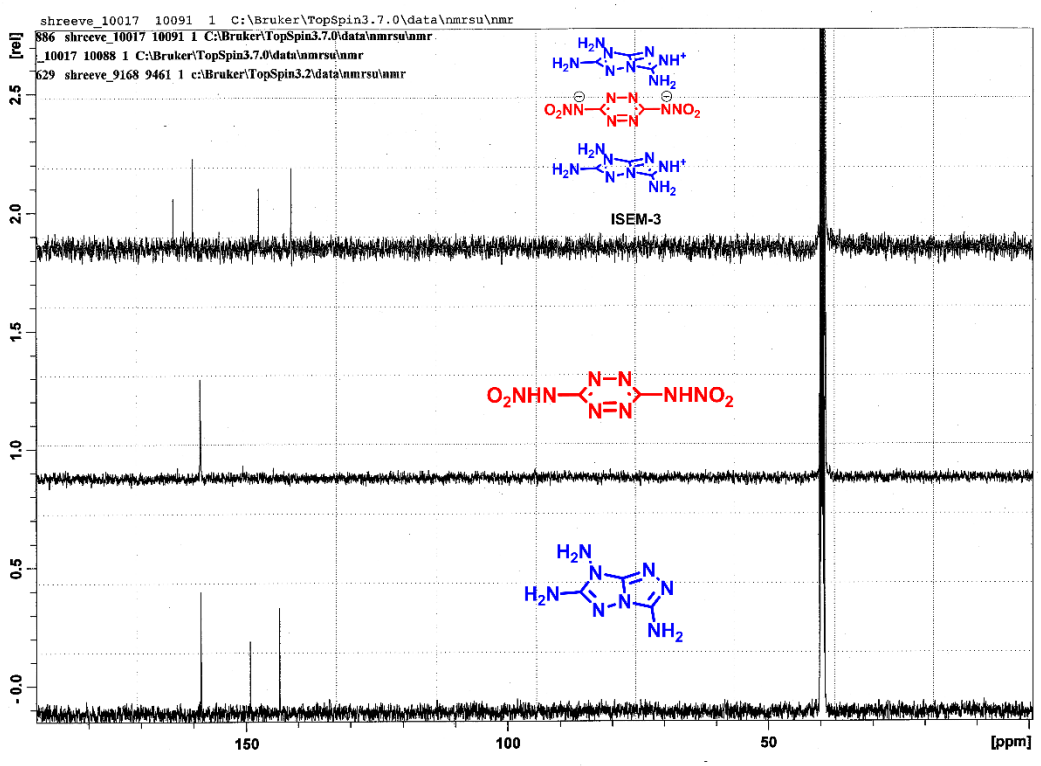


**Figure S40**: $^{13}$C NMR spectra (stacked) for compounds **ISEM-3**, **1** and **TATOT**.

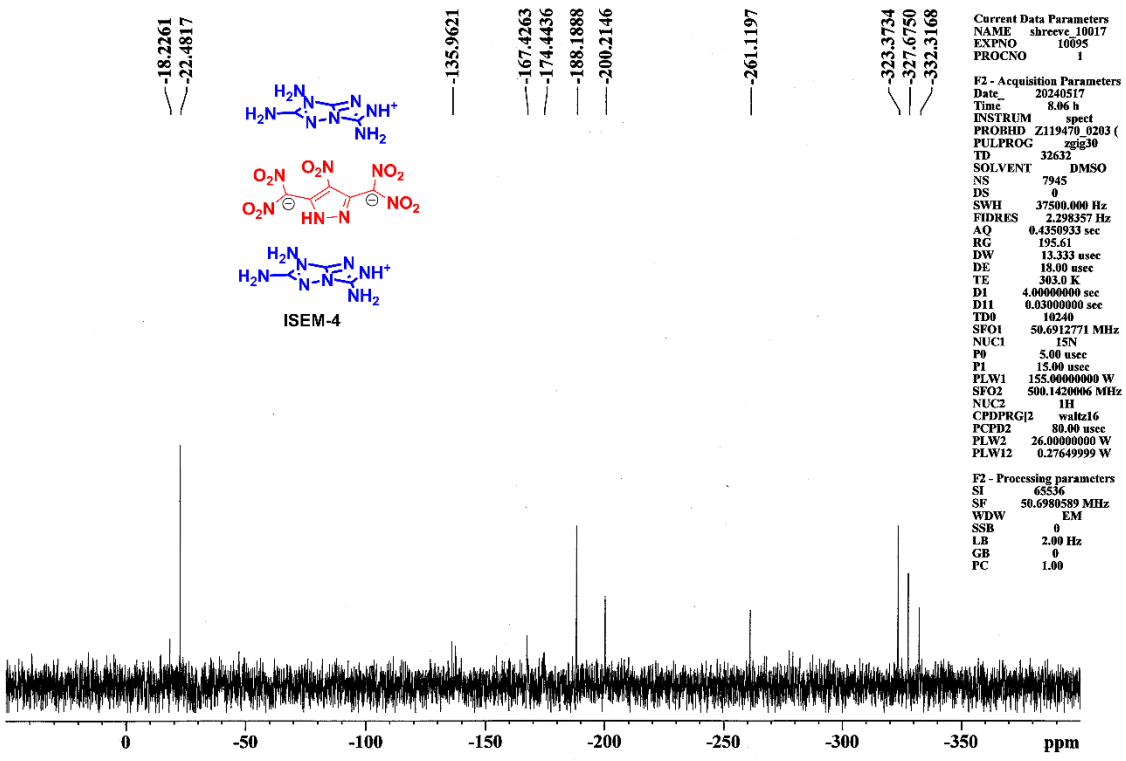


**Figure S41**: $^{15}$N NMR spectrum of compound **ISEM-4**.

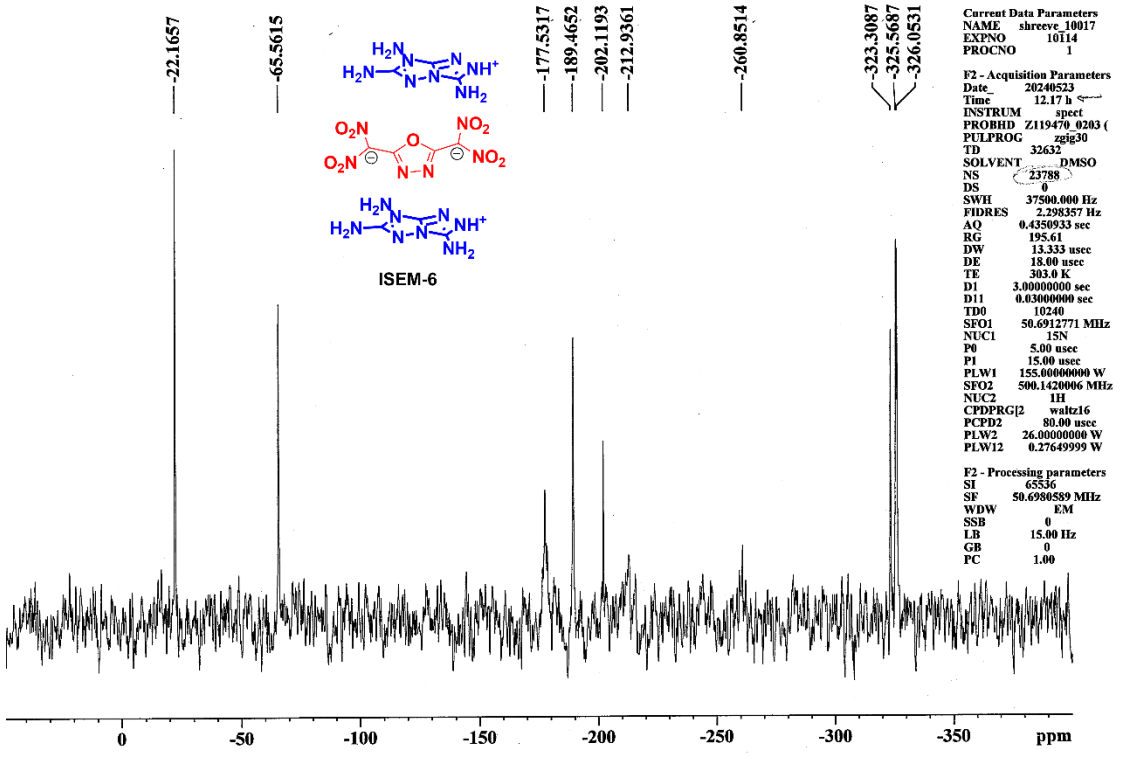


**Figure S43**: $^{15}$N NMR spectrum of compound **ISEM-6**.

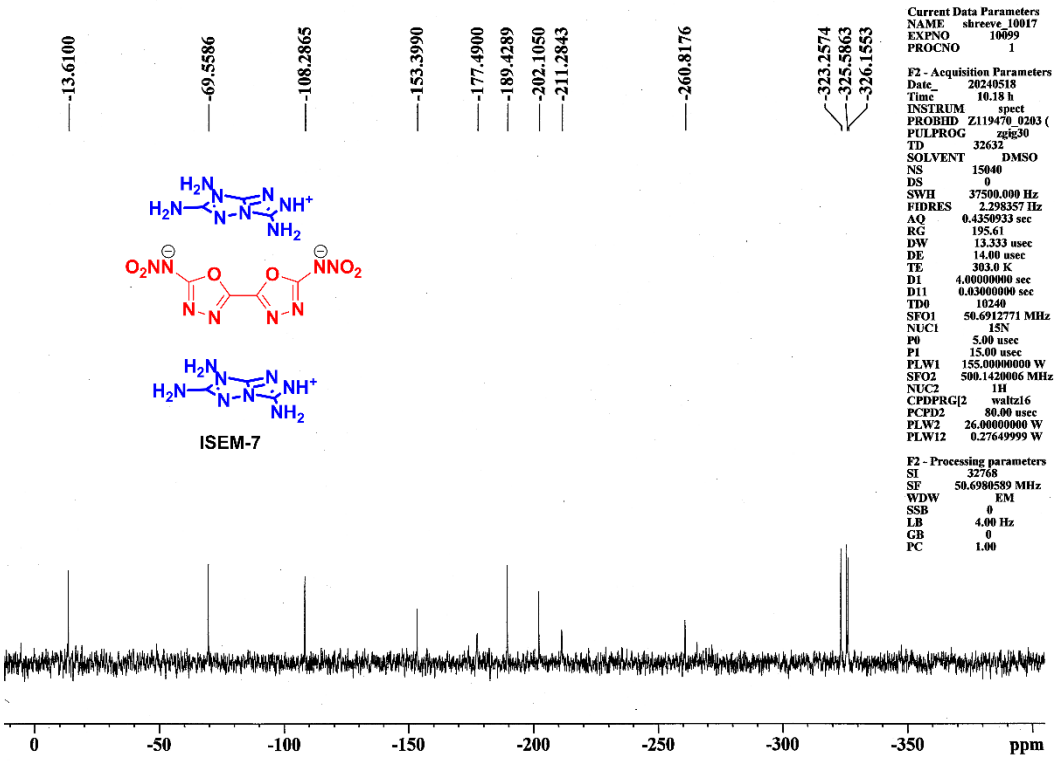


**Figure S42**: $^{15}$N NMR spectrum of compound **ISEM-7**.